ABSTRACT

THE ROLE OF BUTYRYLCHOLINESTERASE IN β-AMYLOID FORMATION IN NEUROBLASTOMA CELLS

By

Lauren K. Hartman

May 2015

Alzheimer's Disease (AD) is a progressive neurodegenerative disease characterized by the formation of insoluble neurotoxic β-amyloid (Aβ) plaques and loss of cognitive function. Plaques have been shown to co-precipitate with both acetylcholinesterase (AChE) and butyrylcholinesterase (BuChE). Interestingly, there is a dramatic increase in BuChE activity relative to AChE in AD patients. Neuroblastoma cells were used to determine the effect of di-*n*-butyl 2-chlorophenyl phosphate (DBPP), an irreversible inhibitor of BuChE, on formation of Aβ. Cells cultured in 10 μM DBPP accumulated significant amounts of the compound without an effect on cell proliferation, membrane integrity, or induction of apoptosis. The intracellular level of BuChE activity was reduced and there was a decrease in amyloid precursor protein (APP) levels. In contrast, there was a concomitant increase in the levels of both Aβ40 and Aβ42 peptides. The implication is that irreversible inhibition of BuChE activity may increase the rate of Aβ formation.

THE ROLE OF BUTYRYLCHOLINESTERASE IN β-AMYLOID FORMATION IN NEUROBLASTOMA CELLS

A THESIS

Presented to the Department of Chemistry and Biochemistry

California State University, Long Beach

In Partial Fulfillment

of the Requirement for the Degree

Master of Science in Biochemistry

Committee Members:

Roger A. Acey, Ph.D.
Douglas D. McAbee, Ph.D.
Kensaku Naykayama, Ph.D.

College Designee:

Chris Brazier, Ph.D.

By Lauren K. Hartman

B.S., 2010, University of California, Santa Barbara

May 2015

ProQuest LLC.
789 East Eisenhower Parkway
P.O. Box 1346
Ann Arbor, MI 48106 - 1346

ACKNOWLEDGEMENTS

I would like to acknowledge the following people whose support greatly contributed to the completion of my thesis. Dr. Roger A. Acey, his guidance and insistence on "work ethic" has kept me motivated throughout my time spent here. I have learned so much and am thankful to have had his guidance throughout my research. I am incredibly thankful for the members of the Acey lab, especially Joselyn Del Cid, Archie Turner, and Josh Feng who were always there to help. They made lab not only a positive place to be, but fun as well. I would also like to thank Paul Madera, Andrew Parker, and Wendy Beck for their advice and support. I am grateful to Dr. McAbee and Dr. Nakayama for reviewing this work. Thank you to my graduate advisor, Dr. Weers, whose support made the completion of this thesis possible. Thanks to Rich Gossett and the IIRMES Lab for their help with GC/MS analysis and the students of Dr. Nakayama's lab for the synthesis of the compounds used in this study. And lastly, I want to thank my parents Jim and Christine, whose love and encouragement kept me going through all the times when I did not think there was a light at the end of the tunnel. I truly appreciate everything you have done for me and dedicate this thesis to you.

TABLE OF CONTENTS

CHAPTER Page

LIST OF TABLES

TABLE Page

LIST OF FIGURES

LIST OF ABBREVIATIONS

1,2-DCB	1,2-diclorobenzene
AChE	Acetylcholinesterase
AD	Alzheimer's Disease
Aβ	Beta-Amyloid
APP	Amyloid Precursor Protein
AICD	APP Intracellular Domain
BuChE	Butyrylcholinesterase
CD	Circular Dichroism
CTD	Carboxyl-Terminal Domain
CTF	Carboxyl-Terminal Fragment
CNS	Central Nervous System
EDTA	Ethylenediaminetetraacetic acid
DBPP	Di-*n*-Butyl 2-Chlorophenyl Phosphate
DEPP	Diethyl 2-Chlorophenyl Phosphate
DBP	Di-*n*-Butyl Phthalate
D-PBS	Dulbecco's Phosphate Buffered Saline
ELISA	Enzyme Linked Immunosorbent Assay
EBSS	Earl’s Balanced Salts Solution
FBS	Fetal Bovine Serum

GC/MS	Gas Chromatography/Mass Spectrometry
IL-1β	Interleukin-1 beta
ILV	Intraluminal Vesicle
kDa	Kilo Dalton
LDH	Lactate dehydrogenase
LDS	Lithium Dodecyl Sulfate
LSM	Low Serum Media
MEM	Minimal Essential Medium
MES	2-(*N*-morpholino)ethanesulfonic acid
P/S	Penicillin/Streptomycin
PAS	Peripheral Anionic Site
PBS	Phosphate Buffered Saline
PRiMA	Proline Rich Membrane Anchor
PKA	Protein Kinase A
ROS	Reactive Oxygen Species
sAPP	Soluble APP Derivative
SDS-PAGE	Sodium Dodecyl Sulfate Polyacrylamide Gel Electrophoresis
siRNA	Small interfering RNA
T/E	Trysin/EDTA (ethylene diamine tetraacetic acid)
T-TBS	Tween-Tris Buffer Solution
TNF-α	Tumor Necrosis Factor-alpha

CHAPTER 1

INTRODUCTION

Cholinesterases (ChEs) belong to a family of serine hydrolases that catalyze the hydrolysis of a variety of substrates. The predominant cholinesterases, acetylcholinesterase (AChE) and butyrylcholinesterase (BuChE), catalyze the hydrolysis of choline esters. AChE is found predominantly in the brain, mainly at neuronal synaptic junctions. BuChE is ubiquitously distributed and found in glial cells, serum, and most body tissues (1,2). AChE has a well-defined function in neurotransmission at cholinergic synapses. The enzyme is responsible for the hydrolysis of the neurotransmitter, acetylcholine. In contrast, the exact role for BuChE is unknown. Although both enzymes are capable of hydrolyzing acetylcholine, AChE is more efficient and is primarily dedicated to acetylcholine hydrolysis in synaptic junctions. AChE and BuChE belong to a super family of proteins that have a common α/β-fold tertiary structure and a conserved active site catalytic triad (2). The catalytic triad consists of three conserved amino acids: a serine, aspartate or glutamate, and histidine. Cholinesterases, unlike serine proteases, have a glutamate residue rather than an aspartate (2,3). The catalytic site in cholinesterases is located near the bottom of a deep gorge, in a type of pocket formed from the folds of β-barrels.

Cholinesterases hydrolyze choline esters though nucleophilic attack by the active-site serine. The substrate is guided into the pocket through interaction with the enzyme's

peripheral site, specifically aspartic acid and tyrosine, which reside at the lip of the active site gorge, directly on the access route to the active site. This site is the first encounter where the substrate interacts with the enzyme. The acyl group of acetylcholine fits in the acyl-binding pocket, composed of hydrophobic residues, while the quaternary nitrogen interacts with the choline-binding site (Trp). Then, catalysis through the catalytic triad can occur (Figure 1).

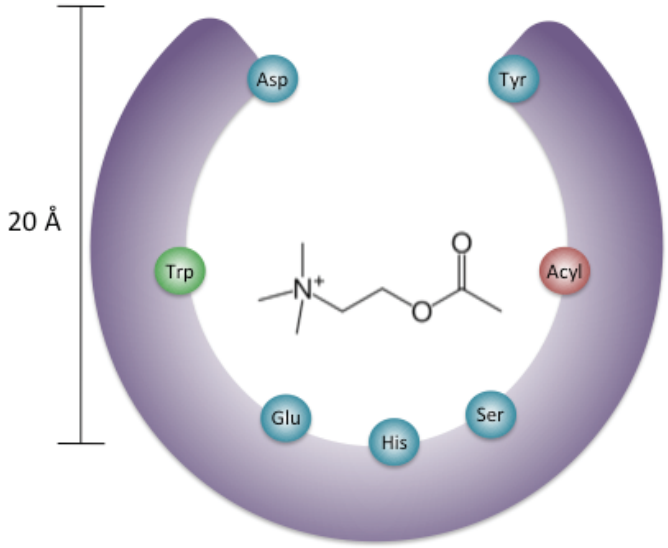

FIGURE 1. Schematic structure of the active site of cholinesterases. Catalytic triad amino acids: serine (Ser), histidine (His), and glutamic acid (Glu); acyl-binding site (Acyl); choline-binding site: tryptophan (Trp); peripheral site: aspartic acid (Asp) and tyrosine (Tyr); substrate: acetylcholine.

Although the mechanism of catalysis is the same between both cholinesterases, the substrate reactivity between the two enzymes are quite different (4). In this respect, size matters. AChE hydrolyzes acetylcholine and small ester compounds, while BuChE hydrolyzes larger molecules such as butyrylcholine. This difference in substrate

reactivity is apparent when considering the structural differences in the catalytic sites between the two enzymes.

The active-site gorge of AChE is lined with fourteen aromatic amino acid residues. The bulky side chains of these residues create a narrow path for the substrate so only small molecules have access to be catalyzed. Six of the fourteen aromatic residues lining the gorge in AChE are replaced with smaller side-chain residues in BuChE, thus allowing for larger substrates (3). For example: BuChE is missing three of the aromatic residues that are present in AChE's peripheral site, creating a wider entry. Additionally, AChE's acyl-binding site consists of two phenylalanine residues, which are replaced with aliphatic residues, leucine and valine, in BuChE (2). These residue replacements in the active-site pocket allow BuChE to accommodate larger substrates.

AChE and BuChE have similar tertiary structures with 55% sequence homology (5). The cholinesterases exist in the brain as soluble and insoluble membrane-bound proteins. The soluble cholinesterases occur as globular catalytic subunits while the insoluble forms are anchored to the plasma membrane via proline-rich membrane anchor (PRiMA) or to the basal lamina via proline-rich attachment domain (PRAD) within a collagen subunit, ColQ (6, 7). ColQ is a collagen-like tail that anchors the tetrameric cholinesterases to the extracellular matrix in the neuromuscular junction. PRiMAs are integral membrane proteins that are able to organize cholinesterases into tetramers and anchor them to the plasma membrane (1,6) (Figure 2). There is evidence supporting the idea that the localization of AChE-PRiMA complexes may influence the enzymes catalytic activity toward acetylcholine (6). Several molecular isoforms are associated with the soluble and membrane-bound cholinesterases, each composed of identical

subunits. G_1 is the soluble monomeric form, G_2 is dimeric, and G_4 is the tetrameric form. G_2 and G_4 exist as soluble as well as membrane-bound proteins. The G_2 form is held together by a disulphide bridge, and the G_4 consists of two G_2 dimers maintained by hydrophobic interactions between seven highly conserved aromatic residues at the C-terminal domain (CTD) of the individual subunits (2,7) (Figure 2).

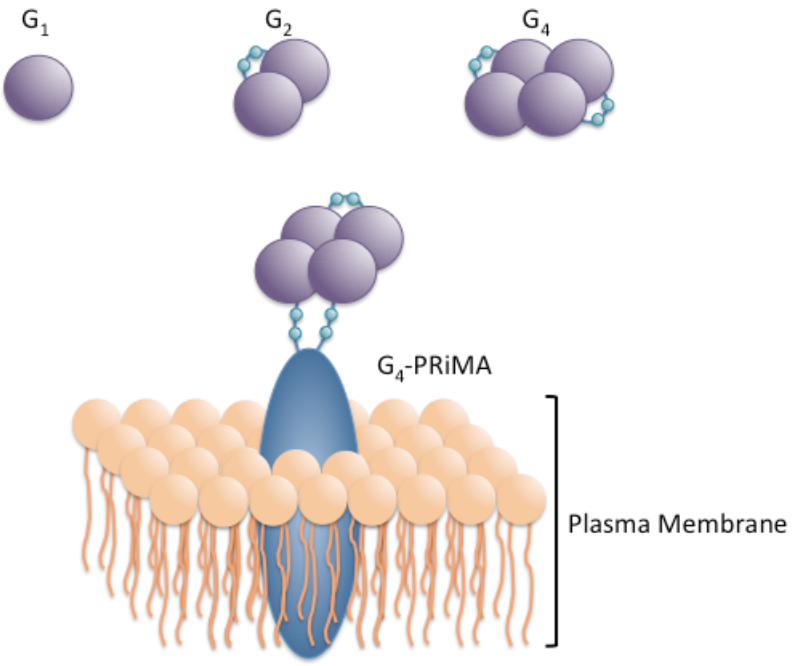

FIGURE 2. Globular forms of cholinesterases. The soluble forms are: monomeric G_1, dimeric G_2, and tetrameric G_4. The insoluble form is a tetrameric G_4 anchored to the plasma membrane (orange layer) via PRiMA (blue oval). Blue hinges represent disulphide bonds.

Although the cholinesterases share similar structures, they demonstrate different localizations and enzymatic characteristics. AChE is located primarily in the brain at neural synapses and neuromuscular junctions where it is bound to the membrane (8).

BuChE is also found in the brain; the brain level of the enzyme, though, is comparatively much lower than other tissues (8). In the brain, BuChE is localized mainly in glial cells, but is present at lower concentrations in neurons and endothelial cells. Interestingly, its activity has been reported within cholinergic synapses in the brain, signifying a role in neurotransmission (9). Although the cholinesterases reportedly localize to separate cellular locations within the brain, cholinergic neurons that express both enzymes suggests a potential relationship between their activities (10).

As noted previously, the exact biological function of BuChE is unknown, but it is capable of hydrolyzing acetylcholine in AChE-knockout mice (10,11). Administration of a BuChE-selective inhibitor in AChE-knockout mice resulted in increased levels of acetylcholine, while the wild-type mice were unaffected (12). This suggests BuChE acts as a "back-up" for AChE in cholinergic nerve transmission. However, BuChE-knockout mice develop normally, adding more confusion to understanding its fundamental role (13). These findings have sparked research to investigate other possible roles of BuChE.

It has been well established that cholinesterases have a fundamental role in regulating the development of the nervous system. BuChE promotes cellular proliferation (13) and influences AChE expression (14). In contrast, AChE promotes cellular adhesion (15), differentiation (16), and neurite outgrowth (17,18).

Layer et al. concluded that BuChE expression precedes that of AChE in developing chicken embryos. High levels of BuChE expression correlated with cell proliferation, while high levels of AChE expression was linked to cell differentiation (13). As the cells proliferated, BuChE expression was high, while AChE expression was low or nonexistent. BuChE expression decreased dramatically as proliferation slowed

and was followed by an increase in expression of AChE accompanied with differentiation of cells and neurite outgrowth (17,19). In another study, anti-sense oligonucleotide inhibition of BuChE expression in developing chicken retinal cells suppressed proliferation and led to an increase in AChE expression that correlated with cellular differentiation (14,16). Furthermore, the same expression trends were shown in a murine embryonic stem cell line (18). Sperling et al. were able to show the expression and coregulation of BuChE and AChE in murine embryonic stem cell differentiation (20). Consistent with the findings of others, BuChE expression levels and enzymatic activity were high at the beginning of differentiation, and down-regulated at later stages while AChE expression levels and enzymatic activity increased over the course of differentiation (20). These studies highlight the direct involvement of the cholinesterases during early neuron development and provide further evidence for BuChE's crucial role during development.

Still, the role of BuChE in development is not only limited to neuronal cells. *In vitro* studies using bone marrow cells showed that changes in BuChE expression interfered with normal development. Antisense oligonucleotide knockdown of BuChE expression inhibited megakaryocytopoiesis and the effect was reversed when exogenous BuChE was introduced (21). These findings further support the importance of BuChE in overall cell differentiation. Along with its role in cellular development, BuChE is also involved in Alzheimer's Disease (AD).

Alzheimer's Disease (AD) is a progressive neurodegenerative disease characterized by the formation of insoluble extracellular Aβ plaques and loss of cholinergic neurons (7). The formation of neurotoxic Aβ interferes with inter-neuronal

communication and eventually causes neuron death (22,23). The depletion of these neurons results in a concomitant reduction of the neurotransmitter acetylcholine, which correlates with a loss of cognitive function in AD patients (8,24). The main components of these plaques are 39-43 amino acid long Aβ peptides that are generated from the proteolytic cleavage of amyloid precursor protein (APP) by a combination of α-, β-, and γ-secretases (25). APP and these secretases are all membrane-bound proteins expressed within neurons, with higher concentrations localized to neuronal synapses (25,26). The resulting peptides accumulate extracellularly in a stepwise process- referred to as amyloidogenesis- to form the neurotoxic Aβ oligomers and eventually the characteristic Aβ plaques (27). Aβ formation is critical in AD, so it is imperative to determine the molecular and cellular basis of its production.

APP is a large type I transmembrane protein with a large N-terminal extracellular domain (ectoderm) and a short C-terminal cytoplasmic domain (Figure 3). APP is ubiquitously expressed as various isoforms within neuronal and non-neuronal tissues. The most predominant isoform contains 695 amino acids and is highly concentrated within neuronal synapses (28). Although the exact role of APP is still unknown, neurotrophic and synaptogenic roles for APP have been reported (29-31). APP may function in synaptic formation and repair and may participate in neurite growth, neuronal migration, and neuroprotection (29,30). Many studies have reported that elevated expression of APP occurs during neuronal differentiation and after neural injury (28,30). In addition, down-regulation of APP is associated with impaired neurite outgrowth and neuronal viability *in vitro* (31), while siRNA-targeted reduction of APP was associated with impaired synaptic activity *in vivo* (32). Furthermore, processing of APP may have

additional roles in neurons. Some studies report that proteolytic fragments may function as signaling molecules that promote axonal growth and regulate cellular communication (33,34).

While the function of APP is not well understood, much is known about its proteolytic processing in AD. APP is sequentially processed through two alternative pathways: In the amyloidogenic pathway, β- and γ-secretase generate, by sequential cleavage, the neurotoxic Aβ peptide, whereas in the non-amyloidogenic pathway, α-secretase cleaves within the amyloid domain and prevents its generation (Figure 3) (29).

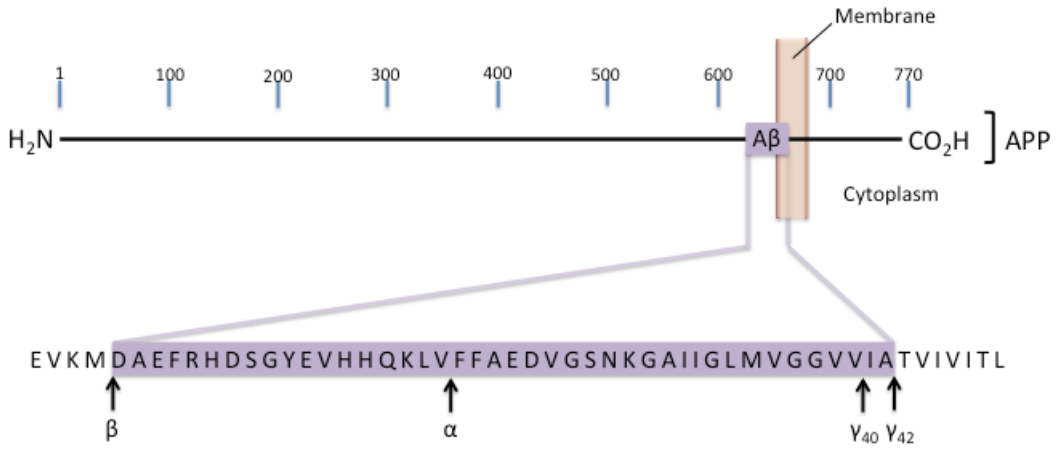

FIGURE 3. Schematic diagram of APP and its cleavage to give Aβ. The length of APP is represented as the predominant isoform consisting of 695 amino acids. α-secretase cleavage site (α); β-secretase cleavage site (β); γ-secretase cleavage site to produce Aβ40 (γ_{40}); γ-secretase cleavage site to produce Aβ42 (γ_{42}).

The formation of these toxic Aβ species from β- and γ-secretase has been extensively studied. β-secretase is the rate-limiting enzyme responsible for the formation of these Aβ

peptides because its knock-out completely inhibits Aβ generation (35). The role of β-secretase and its association with APP to generate Aβ is critical to understanding the disease mechanism.

β-secretase is a type I transmembrane aspartyl protease highly expressed in neurons. It is also found in astrocyte and glial cells, but only under conditions of chronic inflammation, which is typical in neurodegenerative diseases (25,26). It is mainly localized in endosomes, lysosomes, and the trans-Golgi network (28). β-secretase cleaves APP within the extracellular domain, which results in the shedding of the ectodomain to yield a large, soluble APP derivative (sAPP) and a membrane-bound carboxyl-terminal fragment (CTF), the immediate precursor to Aβ (30). Subsequently, γ-secretase, a multi-subunit protease complex, cleaves APP at residues within the transmembrane domain to remove the APP intracellular domain (AICD) and generates amyloid peptides predominantly either 40 (Aβ40) or 42 (Aβ42) amino acids in length (27). γ-secretase cleavage of APP is not restricted to a single site; instead it cleaves APP multiple times in a stepwise process within the transmembrane domain to produce different lengths of Aβ (36). Aβ40 is the most common amyloid isoform while Aβ42 is the amyloidogenic form most often associated with AD. The C-terminal amino acids in Aβ42 are hydrophobic and increase the molecule's susceptibility to conformational changes from an α-helix to an organized β-sheet structure (37). This conformational change plays a role in the process of Aβ fibrillization, which is the accumulation of Aβ peptides to form insoluble fibrils and plaques (Figure 4).

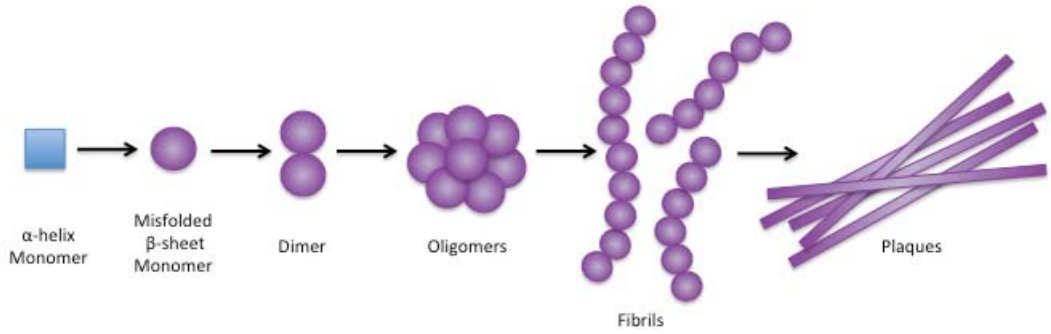

FIGURE 4. Process of Aβ fibrillization. Monomeric Aβ is able to undergo a conformational change to that of a "misfolded" β-sheet structure. These misfolded monomers begin to accumulate to form oligomers and eventually fibrils and plaques.

It is believed that the formation of plaques from the diffuse monomeric peptide is a nucleation-dependent process and is associated with a structural conversion of Aβ from an α-helical structure to that of a β-sheet structure. The fibrillization process begins with a slow lag phase, which is the rate-limiting step in plaque formation: at high concentrations, Aβ undergoes a conformational change to form a β-sheet structure that acts as "seed" to promote assembly into oligomers. Then the growth phase occurs, in which these seeds rapidly develop by further addition of monomers and form larger fibrils and the plaques (Figure 4) (38).

Early endosomes are the major cellular sites for Aβ production (39,40). β-secretase is optimally active in an acidic environment, typically between pH 4-5, thus these compartments provide the low pH required for β-secretase activity (39). If interaction occurs with its substrate, membrane-associated APP, the two proteins are internalized via clathrin-coated pits into early endosomes. Acidification of the vesicle

induces the activation of β-secretase to catalyze the cleavage of APP (41). Once the ectodomain is cleaved, γ-secretase cleavage of APP follows to produce Aβ. After cleavage, the endosomal Aβ is subsequently internalized as intraluminal vesicles (ILVs) of multivesicular endosomes (39). Once the multivesicular endosome fuses to the plasma membrane, the ILVs are released into the extracellular space as exosomes (42). These Aβ-containing exosomes could act as "seeds" for plaque formation by promoting peptide aggregation to form fibrils (43).

Aβ oligomers are more toxic to neuronal cells than mature amyloid plaques (44) and are responsible for the progression of the disease (23,44). The toxic properties of the peptides include synaptic dysfunction (22), mitochondrial damage, microglia activation (23), and neurodegeneration (28). These diffuse peptides are small enough to bind to a receptor on the surface of neurons and modify the structure of the synapse, thereby impairing synaptic plasticity, eventually causing loss of neural synapses (22,45). Shankar et al. sought to determine which forms of soluble Aβ trigger synapse loss. To do this, they examined the effect of Aβ monomers and oligomers on excitatory synapses and dendritic spines in slices of rat hippocampus. Although monomeric Aβ had no effect on neuronal morphology, prolonged exposure to soluble Aβ oligomers induced progressive loss of dendritic spines, accompanied by a decrease in excitatory synapses (22). The study showed that accumulation of these toxic Aβ oligomers caused cellular damage and disrupted critical cellular processes, resulting in toxicity and cell death. Aβ-induced cellular damage, however, occurs through various interactions and the effects on the cell are much more complicated. It is important, therefore, to discern the relationship between Aβ and the molecules involved in its generation.

Cellular damage from Aβ stimulates an inflammatory response, through the activation of microglial cells. Aβ toxicity in turn promotes the production of pro-inflammatory molecules, tumor necrosis factor alpha (TNF-α) and interleukin-1 beta (IL-1β). These molecules reportedly interact with the APP promoter, and enhance its production and processing to produce more Aβ species (46). Additionally, studies have reported Aβ is able to induce and be induced by oxidative stress. Aβ toxicity seems to drive the accumulation of reactive oxygen species (ROS), which then induces increased APP processing to produce Aβ species (47) (Figure 5).

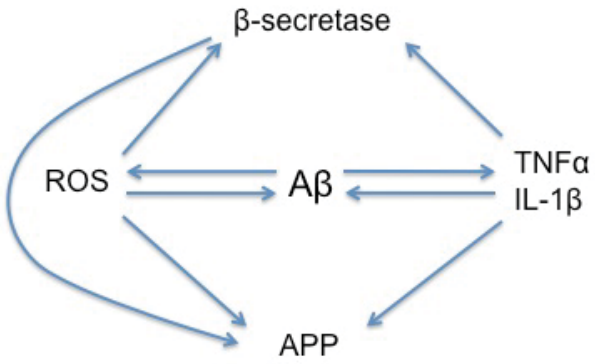

FIGURE 5. Aβ feedback loop. Aβ is at the center of a positive feedback loop, which further elevates the levels of toxic Aβ. ROS, reactive oxygen species; Pro-inflammatory molecules: TNFα, tumor necrosis factor alpha; IL-1β, interleukin-1 beta.

Additionally, several studies have shown that oxidative stress and inflammatory molecules up-regulate the expression of β-secretase (47) while one study suggests that Aβ species directly upregulate β-secretase, although the mechanism remains to be determined. Elevated levels of β-secretase leads to increased APP processing to produce

Aβ species (48). Taken together, oxidative stress and inflammation activate a loop that proceeds with the generation of Aβ peptides. These resulting Aβ peptides play a central role in a positive feedback loop that determines the upregulation of β-secretase and stimulates APP processing through the induction of an inflammatory response as well as the production of reactive oxygen species to further enhance the production of toxic Aβ species (49) (Figure 5).

The accumulation of toxic Aβ peptides, along with other factors, participates in the progression of the neurodegenerative disease. A number of studies have shown that monomeric G_1 AChE and BuChE forms immunoprecipitate with Aβ plaques in AD. Interestingly, abnormal enzymatic activities have been indicated in these complexes: AChE activity is decreased while BuChE activity is increased (50). Although the direct roles the cholinesterases play in Aβ formation are still unknown, there is evidence that shows they may act as molecular chaperones in Aβ formation and influence the process of fibrillization (7,51). Studies have proven AChE's ability to enhance Aβ polymerization and fibril formation (51-53) and increase the toxicity of Aβ to enhance neurodegeneration (54). The AChE motif that promotes Aβ fibril formation is located in a small hydrophobic sequence that contains a conserved tryptophan (W279), which belongs to the peripheral anionic site (PAS) of the catalytic subunit of AChE (53). Using thioflavin-T fluorescence, Bartolini demonstrated that AChE accelerates amyloid polymerization and using circular dichroism (CD) they showed that AChE increases the β-conformation content in Aβ prior to fibril formation (52). Inhibition studies have further elucidated AChE's role in amyloid formation. Cholinesterase inhibitors that block the active site of AChE had no effect on the rate of amyloid formation; however,

inhibitors that block the PAS were shown to reduce the effect of AChE on Aβ fibril formation (51,53). Thus, its pro-fibrillization activity is associated with a site, which lies outside of its catalytic domain.

BuChE also acts as a molecular chaperone in Aβ formation, but unlike AChE, it does not play a role in fibril formation. Instead, BuChE seems to associate with the monomeric form of Aβ through interaction with its CTD to slow the progression of fibrillization. This in turn stabilizes the monomeric Aβ, thus inhibiting its aggregation to form toxic Aβ oligomers and fibrils (55). The G_1 form is drastically increased in the cerebral cortex of AD and correlates with the observed higher concentration of plaques in these brains (9,56). The soluble G_1 form of BuChE has aromatic tryptophans located in its CTD that are capable of forming heteroaromatic complexes with Aβ monomers and oligomers (57). This interaction has been shown to stabilize the monomeric form of Aβ and inhibit propagation of the fibril-formation process to form toxic protofibrils and insoluble fibers (55). Thus, BuChE may act as an attenuator of fibril formation while AChE acts as an enhancer. Interactions between the PAS of AChE and the CTD of BuChE with Aβ indicate the possibility of a protein-protein interaction function of the enzymes (51). BuChE-specific reversible inhibitor studies, however, have shown exactly the opposite effect. Inhibition studies have demonstrated a reduction in the formation of Aβ, indicating that BuChE may have a causal role in Aβ formation (58). Aside from this, it is apparent that these enzymes play a critical role in Aβ formation.

To date, research has been focused on targeting the secretases responsible for the production of Aβ. Unfortunately, development of potential therapeutics has been largely unsuccessful. Thus, research has been investigating alternative approaches for treatment

of AD, such as the cholinesterases, which catalytically act on acetylcholine. Developments of various inhibitors have been found to preserve and maintain the low acetylcholine levels and improve cognitive function (8,11,58).

Currently, there are three cholinesterase inhibitors that are prescribed to treat the cognitive symptoms of AD: Galantamine, Donepezil, and Rivastigmine. Galantamine and Donepezil are highly selective reversible inhibitors of AChE activity. Rivastigmine is a pseudo-irreversible inhibitor of both AChE and BuChE activity; it covalently binds to the enzyme's active site upon cleavage (59). These drugs inhibit cholinesterase activity to reduce the rate of acetylcholine breakdown, resulting in enhanced cognitive function (11,50). However, the effects of reversible inhibitors are dose-dependent since the effects of the drug are based upon their bioavailability and the rate at which they are metabolized and eliminated. This often means that the dosage of the drug is high and administered relatively often. Moreover, they have several off-target effects, alleviate symptoms for only a short period of time, and have no effect on the progressive deterioration of cholinergic nerves.

Although the precise role of BuChE in AD is relatively unknown, studies have suggested a correlation between elevated BuChE activity and increased synthesis of toxic Aβ peptide (58). Recent reports have suggested that selectively inhibiting BuChE, rather than AChE, may prove to be more beneficial in the development of potential treatments for AD (60). Greig et al have shown that selective reversible inhibition of BuChE suppressed the formation of toxic Aβ species (58). The hypothesis here is that irreversible inhibitors of BuChE will also inhibit Aβ peptide expression. Previously, it was shown that aryl dialkyl phosphates are potent and highly selective *irreversible*

inhibitors of BuChE (62). Considering this information, it was of interest to specifically inhibit BuChE using di-*n*-butyl 2-chlorophenyl phosphate (DBPP) and examine the resulting effects on Aβ formation.

CHAPTER 2

MATERIALS AND METHODS

Culture of Neuroblastoma Cells

Human neuroblastoma cells (strain SK-N-SH) were cultured at 37^{o}C and 5% CO_2 in complete Minimum Essential Medium/Earl's Balanced Salts (MEM/EBSS) containing 10% (v/v) FBS, 1% (v/v) Glutamax, and 0.5% (v/v) penicillin/streptomycin. Cells were seeded at a density of 4.0-5.0x10^4 cells/cm^2 in Corning Cell Bind flasks and allowed to grow to 80-90% confluence (four to five days). Spent medium was removed and cells were washed with Dulbecco's Phosphate-Buffered Saline (DPBS; 137 mM NaCl, 8.1 mM Na_2HPO_4, pH 7.4). Three milliliters of Trypsin/EDTA (T/E; 0.05% Trypsin, 0.02% Na_4EDTA) was added to the flask and incubated at 37^{o}C for 5-7 min. Two volumes of complete MEM/EBSS were added to neutralize the trypsin. The cell density was determined using either a hemacytometer or Sceptor 2.0 Handheld Automated Cell Counter (Millipore).

Sterility of DBPP Solutions in Methanol

To determine the sterility of DBPP solutions, an aliquot was streaked on an LB agar plate and incubated at 37^{o}C for 24 hrs.

Toxicity of DBPP/DEPP in Neuroblastoma Cells

For cell viability assays, cells were plated in clear (absorbance measurements) (Corning) or black-walled (for fluorescence measurements) (BRANDplates) 96-well

plates at a density of 40,000 cells per well in complete MEM/EBSS medium and cultured for 24 hrs. Inhibitor solutions were prepared by dissolving DBPP in methanol to a final concentration of 1 mM and diluting into Low Serum MEM/EBSS medium (0.5% FBS and 1% Glutamax) (LSM) to final concentrations of 0.01, 0.1, 1, 10, and 100 μM DBPP. The final methanol concentration was 1% (v/v) methanol. DEPP (0.1 M in methanol) was diluted into LSM to yield final concentrations of 0.01, 0.1, 1, and 5 mM DEPP in 1% (v/v) methanol. Spent medium was replaced with appropriate dilutions of DBPP in LSM and incubated for 24 h at 37°C. The negative control was 1% (v/v) methanol in LSM; LSM alone was used as the blank. The cells were analyzed for cell viability, membrane integrity, and apoptotic induction. All samples were assayed in triplicate and analyzed by ANOVA. P values represent samples compared to the vehicle control.

Cell Proliferation

Cell proliferation was monitored by measuring the absorbance of formazan formation from 3-(4,5-dimethylthiazol-2-yl)-5-(3-carboxymethoxyphenyl)-2-(4-sulfophenyl)-2H-tetrazolium (MTS) using the CellTiter 96 AQueous One Cell Proliferation Assay (Promega). Cells were plated in clear 96-well plates and after exposure to either compound for 24 h, 20 μL of CellTiter96 Reagent was added to each well and incubated in the dark at 37°C for four hours. Results were expressed as the change in absorbance at 490 nm. The change in absorbance is proportional to the rate of cell proliferation.

Membrane Integrity

Membrane integrity was determined with CytoTox-One Homogeneous Membrane Integrity Assay (Promega). Cells were plated in black-walled 96-well plates and after

exposure to either compound for 24 h in LSM at 37°C, the plate was placed at room temperature (25°C) for 30 min. Then 100 µL of CytoTox-ONE reagent was added to each well and incubated at room temperature for 10 min. Then 50 µL of stop solution was added to each well. Fluorescence was measured with an excitation wavelength of 560 nm and emission wavelength of 590 nm. The positive control was 2% (v/v) lysis solution in LSM. This represents complete loss of membrane integrity and maximum LDH activity. The change in fluorescence is a function of increased membrane permeability.

Induction of Apoptosis

Induction of apoptosis was determined with Apo-ONE Homogeneous Caspase-3/7 Assay (Promega). Cells were plated in black-walled 96-well plates and after exposure to either compound for 24 h, 100 µL of Apo-ONE reagent was added to each well and incubated at room temperature (25°C) for 18 h. Fluorescence was measured using an excitation wavelength of 499 nm and emission wavelength of 521 nm. The positive control was 1 µM Staurosporine in LSM, which represented maximum induction of apoptosis. The change in fluorescence of each sample reflects an increase in apoptotic activity.

Cell Proliferation with Methanol

Cells were plated in a 96-well plate at a density of 40,000 cells per well in complete MEM/EBSS medium and maintained for 24 h. Methanol was diluted in LSM to give final concentrations of 0.5%, 1%, and 2% (v/v) methanol in LSM. Spent medium was replaced with appropriate dilutions of methanol in LSM and incubated for 24 h at 37^{o}C. LSM alone was used as the blank. All samples were assayed in triplicate. The

cells were analyzed for cell viability using CellTiter 96 AQueous One Cell Proliferation Assay (Promega).

Stability of DBPP in Low-Serum Media

Ten milliliters of LSM containing 10 µM DBPP was incubated at 37°C for 0, 4, and 24 h. After incubation for the various time periods, 10 µL of 1,2-dichlorobenzene (1,2-DCB) was added to the solution. 1,2-DCB was used as a recovery surrogate to monitor extraction efficiency because it has similar structural characteristics and chemical properties as DBPP. The solution was extracted with 1.5 ml of dichloromethane (DCM). The extract was then dried over 0.55 g of anhydrous magnesium sulfate. Each extraction was performed in triplicate. Extracts were analyzed by GC/MS. One hundred microliters of Anthracene-d10 was added to each sample as an internal standard before GC/MS analysis to quantify amounts of 1,2-DCB and DBPP. Amounts of the two compounds were quantified using a five point standard curve. The corrected amount of DBPP was obtained using Equation 1.

$$\text{Corrected µg DBPP} = \text{µg DBPP}_{\text{GC/MS}} \times \left(\frac{\text{µg 1,2-DCB}_{\text{added}}}{\text{µg 1,2-DCB}_{\text{GC/MS}}}\right) \qquad \text{Equation 1}$$

Uptake of DBPP

Cells were cultured in Corning T25 Cell Bind flasks as described previously with the following changes. DBPP was added to LSM to a final concentration of 10 µM. Cells were incubated at 37°C, 5% CO_2 for 0, 4, and 24 h. Three different flasks were collected for each time point. The cells were collected, pelleted by centrifugation at 1800 RPM, 18°C for 10 min, and washed three times with DPBS. 1,2-DCB was added to the cell pellet to monitor the extraction efficiency and the cells were extracted with DCM. The extracts were dried over anhydrous magnesium sulfate. Each sample was extracted

three times and the extracts pooled. Anthracene-d10 was added as an internal standard and the extracts were analyzed by GC/MS for 1,2-DCB and DBPP. Amounts of the two compounds were quantified using a five point standard curve. The amount of DBPP was recovery corrected using Equation 1.

Cell Culture with DBPP

Cells were cultured in complete medium as described above. Spent medium was removed and the adherent cells washed with DPBS. A solution of 1 mM DBPP in methanol was diluted with LSM to a final concentration of 10 μM in 1% methanol. The solution was mixed well and added to culture flasks. LSM containing 1% (v/v) methanol served as the control. Cells were collected immediately for the 0 h time point or collected after culturing for 24 h at 37^{o}C, as described previously. Cell pellets were washed three times with DPBS, centrifuged at 1800 RPM and 18^{o}C for 10 min, and stored as pellets at -80^{o}C.

Cell Homogenization

Cell pellets were thawed and resuspended in either 5% (v/v) glycerol, 10 mM β-octyl glucopyranoside (OGP), DPBS, pH 7.4, and 2.5 μL of protease inhibitor cocktail (Sigma) or RIPA (1% (v/v) Nonidet P40 (NP40), 0.5% (w/v) sodium deoxycholate, 0.1% SDS, DPBS, pH 7.4) and 2.5 μL of protease inhibitor cocktail (Sigma), at a ratio of 1 mL of buffer per 1.0x10^{7} cells. The cells were homogenized in a 2 mL Dounce Homogenizer and then placed on ice for 30 min. The extracts were centrifuged at 4^{o}C and 10,000 RPM for 10 min. Protein concentration of the supernatants using OGP containing buffer was determined using a Coomassie (Bradford) Protein Assay (Pierce); for the samples

homogenized in RIPA, protein concentration was determined using a bicinchoninic acid (BCA) colorimetric assay (Pierce).

Effect of DBPP on Cellular Butyrylcholinesterase Activity

Cells were cultured with or without 10 μM DBPP in LSM as described previously for uptake of DBPP with the following changes. Cells were plated at a density of 5.25x105 cells/cm^2. After 24 h exposure to DBPP, cells were collected and homogenized in OGP buffer at a ratio of $5.0x10^6$ cells per mL of buffer as described previously. Extracts were transferred to a 30K Amicon Ultra Centrifugal Filter (Millipore) and spun at 4000 x g at 4°C for 15 min. The concentrate was washed twice, each with 5 mL of 5% (v/v) glycerol in DPBS. The resulting concentrate was collected and analyzed for BuChE activity.

Butyrylcholinesterase Activity Assay

True butyrylcholinesterase activity was determined by incubating samples with or without tetra isopropyl pyrophosphoramide (iOMPA, Sigma), a selective irreversible inhibitor of BuChE. A solution of 10 mM iOMPA in distilled water was added to extracts to a final concentration of 100 μM and incubated on ice for 30 min. A commercially available assay, BuChE Fluorescent Activity Kit (Arbor Assays), was used to measure BuChE activity. The kit utilizes a proprietary non-fluorescent molecule, ThioStar®, that covalently binds to the thiol product of the reaction between butyrylthiocholine and BuChE, generating a fluorescent product.

Extracts were mixed with an equal volume of assay buffer. Then, 100 μL of the dilution was added to a 96-well plate (Corning). Fifty microliters of the reaction mixture was added to each sample well and the plate incubated at room temperature for 20 min.

Assay buffer served as the blank. Fluorescence was measured using an excitation wavelength of 390 nm and emission wavelength of 510 nm. Fluorescent values are proportional to the relative amount of BuChE activity present in the samples. The results were converted to mU of BuChE activity per mg of protein.

The relative amount of true BuChE activity inhibition was determined by taking the difference of samples treated with iOMPA from the same time point samples without iOMPA (Table 1 and Equations 2-5). This difference gives the relative amount of true BuChE activity in the samples at that particular time point.

TABLE 1. BuChE Activity Calculation Table

	A	**B**	**C**
	(-) iOMPA	100 μM iOMPA	Difference (A-B)
24 h	X	X_i	$X-X_i$
DBPP	X_{DBPP}	X_{i+DBPP}	$X_{DBPP}-X_{i+DBPP}$

Amount of BuChE activity, X. Amount of BuChE activity from iOMPA inhibition, X_i. Amount of BuChE activity from DBPP inhibition, X_{DBPP}. Amount of BuChE activity from iOMPA and DBPP inhibition, X_{i+DBPP}.

Amount of inhibition from iOMPA at 24 h (i)

$$X - Xi = i \qquad \text{Equation 2}$$

Amount of inhibition from iOMPA during treatment with DBPP at 24 h (i+$DBPP_i$)

$$X_{DBPP} - X_{i\,+\,DBPP} = i + DBPP_i \qquad \text{Equation 3}$$

Amount of true inhibition of BuChE from DBPP only ($DBPP_i$)

$$i - (i + DBPP_i) = DBPP_i \qquad \text{Equation 4}$$

Percent BuChE activity inhibition

$$\%\ \text{BuChE activity inhibition} = \frac{DBPP_i}{i} x\ 100\% \qquad \text{Equation 5}$$

Quantification of APP by Western Blotting

Cells were cultured with or without 10 μM DBPP in LSM for 0 and 24 h. Spent medium was replaced with fresh medium containing 10 μM DBPP after 4 and 8 h of culture. After 24 h, the cells were collected, pelleted by centrifugation at 1800 RPM, 18^{o}C for 10 min, washed, and lysed in RIPA buffer, as described above. Two separate western blot procedures were performed to validate test results.

In the first procedure (Procedure 1), a volume of extract containing 10 μg of protein was mixed with an equal volume of Laemmli sample buffer (BioRad) containing 5% (v/v) β-mercaptoethanol (βME) (Sigma) and heat denatured at 95^{o}C for 10 min. Samples were loaded onto a Tris-HEPES NH 4-20% gel (NuSep) and fractionated at 150 V for 45 min using 1.2% (w/v) Tris, 2.5% (w/v) HEPES and 0.1% (w/v) SDS as running buffer. Pre-stained Protein Marker (Kaleidoscope, BioRad) was used as a molecular weight standard. Three microliters of Magic Mark XP (Invitrogen) was used as a positive control.

Proteins were transferred onto nitrocellulose (GenScript 0.2 μm pores) overnight at room temperature and 19 V using 0.3 mM sodium carbonate, 8 mM sodium bicarbonate, and 10% (v/v) methanol as transfer buffer.

Detection of APP was accomplished using a one-step western blot kit (GenScript). All necessary reagents, buffers, and materials were provided in the kit. The primary antibody was monoclonal anti-APP A4 antibody (MAB348, Millipore) that recognizes amino acids 66-81 of the N-terminus on the APP protein ectodomain.

The nitrocellulose membrane was blocked using a pretreatment solution and then incubated in the anti-APP antibody (1:5000 dilution) for 60 min at room temperature. The membrane was washed three times with wash solution, provided in the kit, and exposed to LumiSensor chemiluminescent HRP substrate for five min in the dark. Signals were detected by exposing the membrane to high-sensitivity X-ray film and the film was developed.

In the Procedure 2, an aliquot of extract containing 10 µg of protein was mixed with an equal volume of LDS Sample Buffer (NuPAGE) containing 10% (v/v) sample reducing reagent (NuPAGE) and heat denatured at 90^{o}C for 5 min. Samples were loaded onto a precast SDS/PAGE 10% Bis-Tris gel (NuPAGE) and run at 200 V for 40 min using 50mM MES, 50mM Tris Base, 0.1% (w/v) SDS, and 1mM EDTA, pH 7.3 as running buffer. SeeBlue Plus2 Pre-Stained Standard (Invitrogen) was used as a molecular weight standard.

Proteins were then immediately transferred onto nitrocellulose (Novex 0.2 µm pores) using an iBlot Dry Blotting System (Invitrogen) and transferred for seven minutes.

Membranes were then incubated in a 5% non-fat dried milk powder in T-TBS (0.02% Tween 20, 100 mM Tris pH 7.5; 150 mM NaCl) for 1 h at 25 ºC. Detection of APP was accomplished using the monoclonal anti-Aβ antibody 6E10 (Covance) that recognizes an epitope of amino acids 3-8 of Aβ. Covance's beta amyloid antibody 6E10 reacts to the abnormally processed isoforms, as well as precursor forms (APP). Polyclonal rabbit β-Actin (Sigma) was used as the loading control. The membrane was then incubated in 6E10 antibody (Covance) (1:2000) and β-Actin (Sigma) (1:10,000) overnight at 4ºC. Membranes were washed three times in T-TBS for a total of 30

minutes and incubated in goat anti-mouse IRDye 680LT or goat anti-rabbit IRDye 800CW LI-COR secondary antibodies (1:10,000) for 1 hour at 25 ºC. After three final washes, membranes were imaged and analyzed using the LI-COR Odyssey (LI-COR, Lincoln, Nebraska). Protein densitometry was calculated by dividing the integrated intensity of APP by the integrated intensity of β-Actin loading control, both obtained using the LI-COR Odyssey software. To confirm the results of the signal obtained from 6E10, the anti-APP A4 antibody MAB348 (Millipore) was used.

Quantification of Aβ by ELISA

Cells were cultured with or without 10 μM DBPP in LSM for 24 h, without replacement of media. Cells were plated at a density of $5.25x10^5$ cells/cm^2 in a 6-well plate (CoStar). After 24 h, spent medium was collected and immediately stored at -20^{o}C. The samples were thawed on ice and concentrated in 2K filter columns (VivaSpin) at 4000 X G and 4^{o}C for 40 min. The concentrate was then washed twice with DPBS. Total protein of the concentrated samples was determined with Coomassie (Bradford) Protein Assay (Pierce).

The concentrated medium was then analyzed for Aβ40 and Aβ42 peptides using a commercially available ELISA kit (Millipore) following the manufacturer's protocol. Sample Diluent served as the blank. The amount of Aβ was quantified from a five-point standard curve. The assay was considered acceptable when all values for the Quality Control (QC) samples fell within the calculated QC range, provided for each kit. The relative amount of Aβ peptide was expressed as picograms of amyloid peptide per milligram of protein.

CHAPTER 3

RESULTS

Toxicity, Stability and Cellular Uptake Studies of DBPP

Previous studies have demonstrated that aryl dialkyl phosphates are potent irreversible inhibitors of BuChE (50). The inhibitory activity of the compounds was tested against AChE, chymotrypsin, trypsin, hexokinase and PKA and shown to have no effect on the enzymes (62). The potential advantage of targeting Aβ peptide formation with irreversible BuChE inhibitors is diminished side effects, extended pharmacological effects at a lower dosage, and a longer period between doses. Therefore, the potential of these compounds as inhibitors of Aβ formation was tested with human neuroblastoma cells.

Sterility of DBPP Solutions

To ensure any pharmacological effects were not due to bacterial contamination of the inhibitor stock solution, the sterility of DBPP was determined by standard microbiological techniques. An agar plate was streaked with a 100 µl aliquot of 10 mM DBPP in methanol and placed in a incubator at 37°C. There were no visible bacterial colonies after twenty-four hours of culture. Thus, the solution was determined to be sterile.

Toxicity Studies of DBPP on Neuroblastoma Cells

Control cultures contained methanol, the solvent used to solubilize the DBPP. To assess the effect of methanol on cellular proliferation, neuroblastoma cells were treated with various concentrations of methanol (0.5% to 2%). Cells cultured with 1% methanol showed little to no effect on cellular proliferation, relative to the control containing low serum medium (LSM) without methanol (Figure 6). Cells incubated with the various methanol treatments were statistically different than the control, $P < 0.05$ (ANOVA), but no significant difference was found between the methanol test samples.

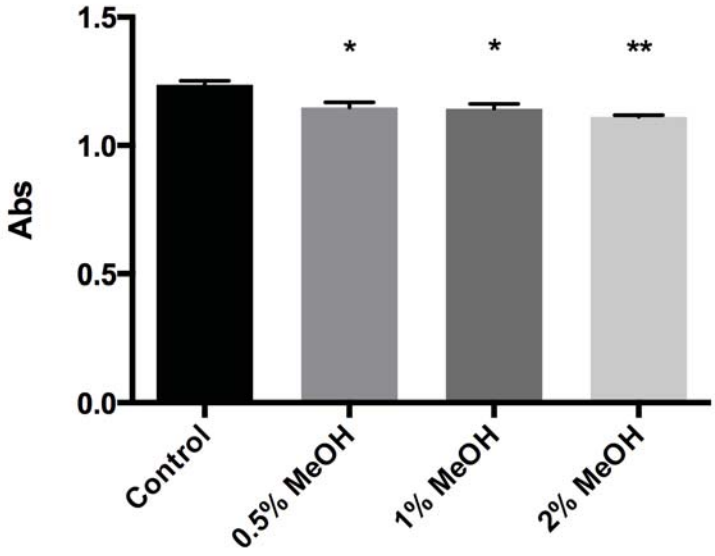

FIGURE 6. Effect of methanol on cellular proliferation. Control, LSM only. Results are expressed as the mean of three replicates ±SEM. Asterisk indicates a significant effect of methanol on proliferation vs. LSM control (*$P < 0.05$ and **$P < 0.005$, ANOVA).

The maximum concentration of DBPP that cells could tolerate after 24 hours of culture without affecting their viability was then determined as described in Materials and Methods.

DBPP at concentrations ranging from 0.01 μM to 10 μM had no effect on cell proliferation when compared to the methanol control ($P > 0.1$, ANOVA). There was no statistical difference between 0.01 μM to 10 μM treatment samples. However, 100 μM of DBPP was significantly toxic to cells ($P < 0.0001$, ANOVA) (Figure 7).

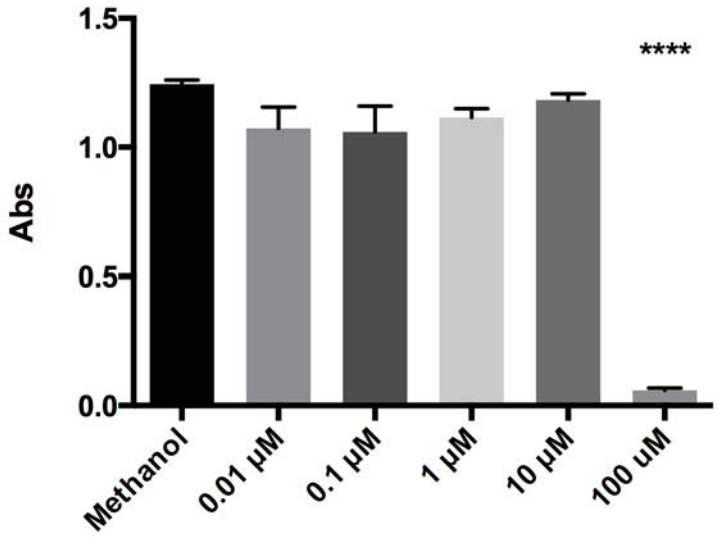

FIGURE 7. Effect of DBPP on cellular proliferation. Solvent control, 1% Methanol. Results are expressed as the mean of three replicates ±SEM. Asterisk indicates a significant effect on proliferation vs. methanol control (****$P < 0.0001$, ANOVA).

In addition, the effect of DBPP at concentrations between 0.01 μM and 10 μM had no effect on membrane integrity (Figure 8) or induction of apoptosis compared to methanol control (Figure 9) ($P > 0.1$, ANOVA). There was no statistical difference between 0.01 μM to 10 μM treatment samples. However, 100 μM of DBPP had a significant effect on membrane integrity ($P < 0.0001$) and enhanced apoptotic induction when compared to the vehicle control ($P < 0.0001$) (ANOVA).

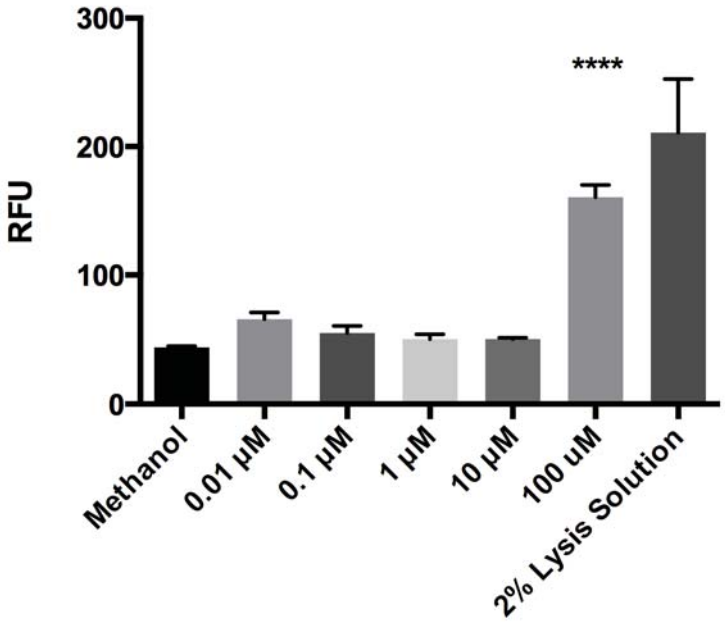

FIGURE 8. Effect of DBPP on membrane integrity. RFU: relative fluorescent units. Solvent Control, 1% Methanol; Positive control, 2% (v/v) lysis solution. Results are expressed as the mean of three replicates ±SEM. Asterisk indicates a significant effect on membrane integrity vs. methanol control (****$P < 0.0001$, ANOVA).

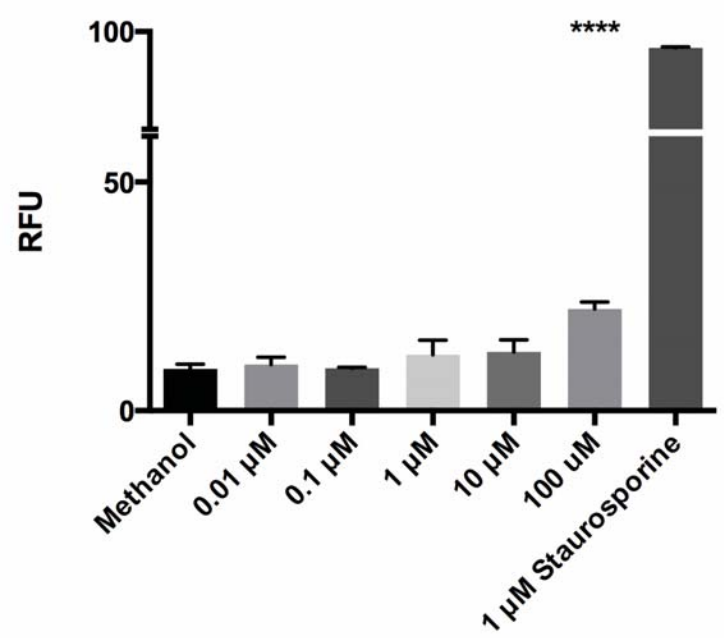

FIGURE 9. Effect of DBPP on apoptotic induction. RFU: relative fluorescent units. Solvent control, 1% Methanol; Positive control, 1µM Staurosporine. Results are expressed as the mean of three replicates ±SEM. Asterisk indicates a significant effect on apoptotic induction vs. methanol (****$P < 0.0001$, ANOVA).

Based on these results, 10 µM of DBPP was used in all subsequent experiments with the neuroblastoma cells.

Once the maximum concentration of DBPP the cells could tolerate was determined, the stability of DBPP was assessed in LSM. FBS in the culture medium contains BuChE; therefore it was necessary to evaluate its effects on the concentration of the compound. LSM was incubated with DBPP, and then extracted immediately, 4, and 24 hours after addition and analyzed by GC/MS. After incubation in LSM for 4 hours, 46.2% of the DBPP was still present (Figure 10). After 24 hours, 32.6% DBPP still remained in the medium. Due to the degradation of the compound, media was replaced with fresh 10 µM DBPP in LSM at 4 and 8 hours after the initial treatment. Replacement

of media was performed for the following experiments: cellular uptake of DBPP, the effect of DBPP on cellular BuChE activity, and the effect of DBPP on cellular APP expression.

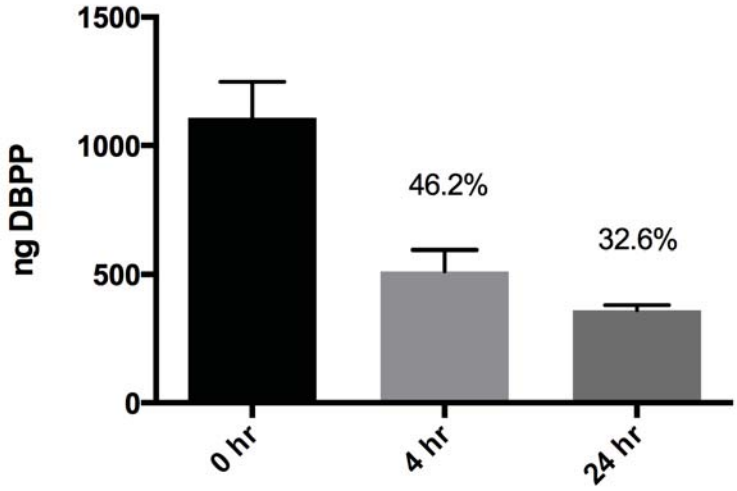

FIGURE 10. Stability of DBPP in LSM. LSM incubated with 10 μM DBPP was collected and extracted as described in Materials and Methods. Results are expressed as the mean of three replicates ±SEM.

Intracellular levels of DBPP after various periods of exposure to neuroblastoma cells was determined to evaluate DBPP's ability to cross the cellular membrane and potentially interact with intracellular BuChE. Cells were cultured in 10 μM DBPP in LSM and the medium replaced with fresh LSM containing 10 μM DBPP at 4 and 8 hours. The cells were collected at the time points indicated, extracted with dichloromethane and analyzed by GC/MS. The amount of DBPP present in cells after 0, 4, and 24 hours of exposure was 37 fg/cell, 60.4 fg/cell, and 82.5 fg/cell, respectively (Figure 11). The results indicate that the cells do in fact take up DBPP.

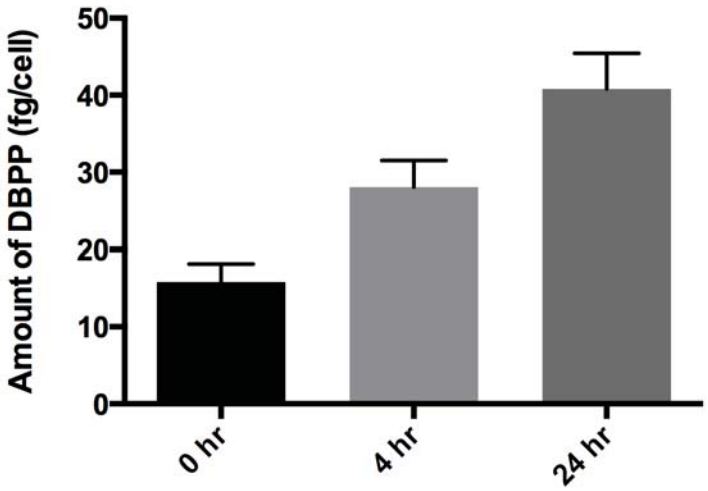

FIGURE 11. Uptake of DBPP into neuroblastoma cells. Cells incubated with 10 μM DBPP were collected and extracted as described in Materials and Methods. Results are expressed as the mean of three replicates ±SEM.

Toxicity Studies of DEPP on Neuroblastoma Cells

The cell toxicity experiments were repeated using diethyl 2-chlorophenyl phosphate (DEPP), a significantly less potent inhibitor of BuChE (62). Neuroblastoma cells were treated with 10 μM, 100 μM, 1 mM, and 5 mM DEPP for 24 hours and analyzed for the effect on cell proliferation, membrane integrity, and apoptotic induction. Concentrations as high as 100 μM DEPP had no effect on cell proliferation (Figure 12), membrane integrity (Figure 13), or induction of apoptosis (Figure 14) when compared to methanol control ($P > 0.05$, ANOVA). There was no significant difference between 10 μM and 100 μM DEPP treatment samples. However, 1 mM DEPP showed diminished cell proliferation, enhanced membrane permeability, and induction of apoptosis compared to methanol control ($P < 0.05$, ANOVA). Therefore, cellular uptake experiments with DEPP and neuroblastoma cells were performed with 100 μM DEPP.

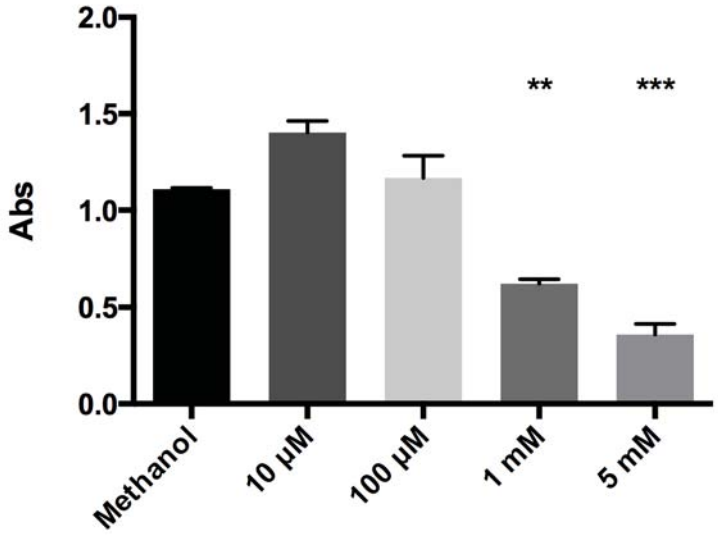

FIGURE 12. Effect of DEPP on cellular proliferation. Solvent control, 1% methanol. Results are expressed as the mean of three replicates ±SEM. Asterisk indicates a significant effect on proliferation vs. methanol control (**$P < 0.01$ and ***$P < 0.001$, ANOVA).

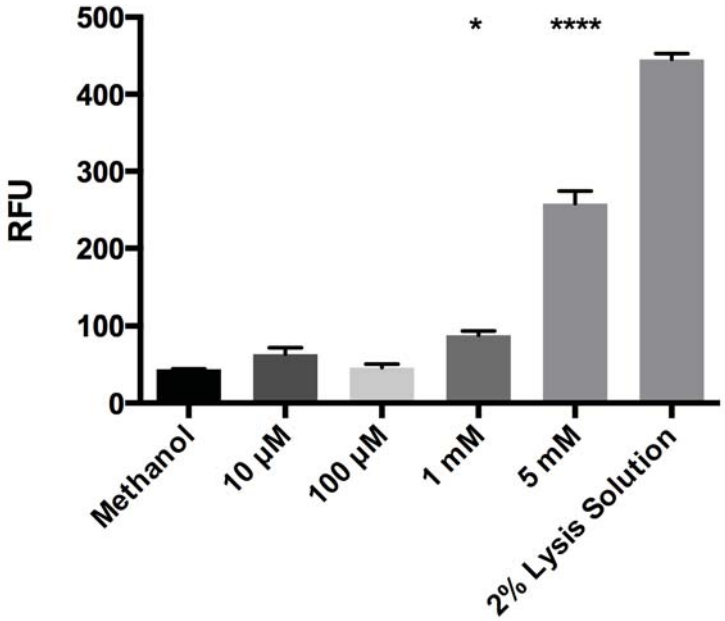

FIGURE 13. Effect of DEPP on membrane integrity. RFU: relative fluorescent units. Solvent control, 1% Methanol; Positive Control, 2% (v/v) lysis solution. Results are expressed as the mean of three replicates ±SEM. Asterisk indicates a significant effect on membrane integrity vs. methanol control (*$P < 0.05$ and ****$P < 0.0001$, ANOVA).

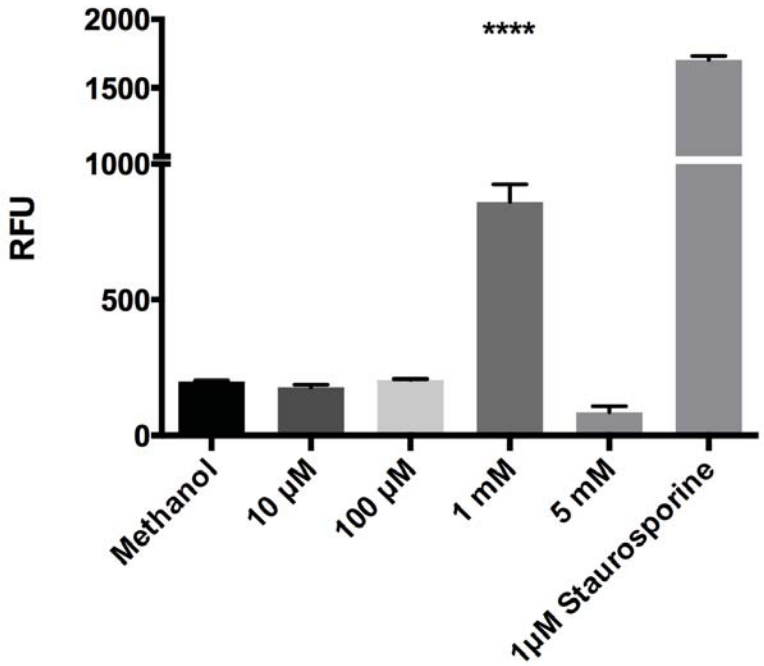

FIGURE 14. Effect of DEPP on apoptotic induction. RFU: relative fluorescent units. Solvent control, 1% Methanol; Positive Control, 1µM Staurosporine. Results are expressed as the mean of three replicates ±SEM. Asterisk indicates a significant effect on apoptotic induction vs. methanol control (****$P < 0.0001$, ANOVA).

To assess the ability of DEPP to pass the membrane, cellular levels of DEPP were measured after different periods of exposure. DEPP was undetectable in cells treated with DEPP for 24 hours. Since cells did not accumulate detectable levels of DEPP, experiments elucidating DEPP's effects on intracellular APP expression and Aβ formation were not performed.

Studies on the Effects of DBPP on BuChE Activity

The next step was to determine if the compound actually inhibits the target enzyme, BuChE. The degree of intracellular BuChE inhibition by DBPP was evaluated at 24 hours. Protein extracts from treated and untreated cells were concentrated to enhance BuChE activity. It was important to ensure that the detergent used in the

extraction buffer did not interfere with the assay. β-octyl glucopyranoside (OGP) is a non-ionic, dialyzable detergent used for the solubilization and isolation of membrane proteins. This detergent was tested and was found to have no interference with the assay. Therefore, the possibility of inhibition from the detergent was ruled out. The 30K Ultra Centrifugal filters allowed for the dialysis of OGP, further ensuring that there were no extraneous interactions of OGP in the assay that might contribute to the signal. iOMPA, a specific irreversible inhibitor of BuChE, was used to determine "true" BuChE activity. The difference in activity between treated and untreated samples with iOMPA is the "true" BuChE activity (Table 2, column C). The amount of "true" BuChE activity was determined using Equations 2-5. In cells cultured for 24 hours without DBPP, the amount of BuChE inhibition by iOMPA was approximately 3.1 mU/mg. In extracts treated with DBPP for 24 hours, the amount of BuChE inhibited by iOMPA was approximately 1.83 mU/mg. The difference of these gives the "true" inhibition of BuChE from DBPP, 1.27mU/mg. It was calculated that approximately 40.97% of BuChE activity was inhibited after treatment with DBPP for 24 hours (Table 2).

TABLE 2. Effect of DBPP on Cellular Butyrylcholinesterase Activity

	A	**B**	**C**
	(-) iOMPA	100 μM iOMPA	Difference (A-B)
0 h	8.75 ± 0.02	5.61 ± 0.06	3.14
24 h	9.74 ± 0.11	6.64 ± 0.05	3.1
DBPP	8.78 ± 0.12	6.95 ± 0.05	1.83

Expressed as mU BuChE activity per mg total protein. Data shown is the mean ± SEM (n=3).

Studies on the Effect of DBPP on Cellular APP Expression and Aβ Formation

The next step was to assess the effect of DBPP on expression of APP and subsequently the formation of Aβ peptide. APP is cleaved to produce Aβ peptides, which aggregate in the process known as fibrillization, to form amyloid plaques. As noted previously, both BuChE and AChE are associated with the plaques. Western blot analysis of APP was performed using two procedures mentioned in materials and methods. In procedure 1, protein extracts from cells treated with 10 μM DBPP showed a decrease in the APP signal relative to untreated samples when probed with MAB348 (Figure 15, A). In procedure 2, protein densitometry was calculated by dividing the integrated intensity of APP by the integrated intensity of β-actin loading control (LI-COR Odyssey Software). Cells treated with 10 μM DBPP revealed a 37.2% reduction in the APP signal relative to the control at 24 hours, when probed with 6E10 antibody (Covance) (Figure 15, B). To confirm these results, MAB348 (Millipore) was used again and revealed a 49.4% decrease in the APP signal in samples treated with DBPP (Figure 15, C). Additional bands detected from the MAB348 immunoblot may be the result of the antibody's nonspecific interactions, as this antibody is known to cross-react with APP-like proteins, such as APLP2 (63).

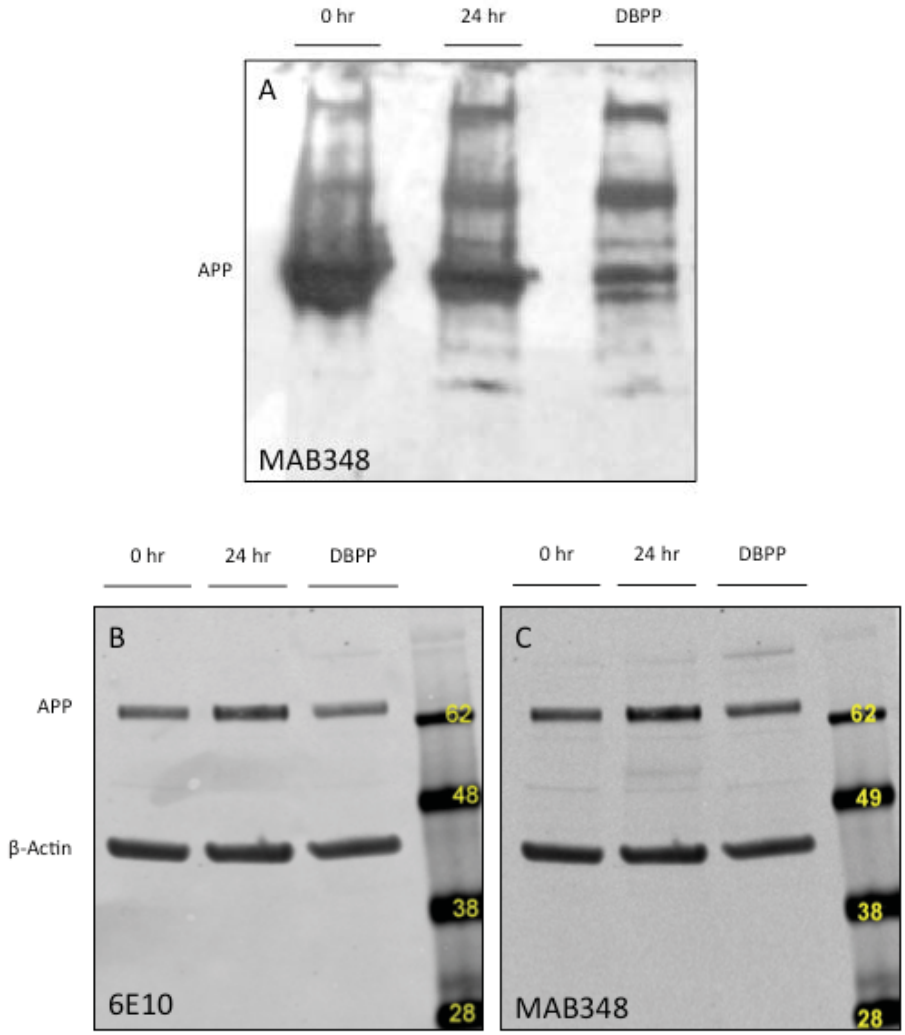

FIGURE 15. Immunoblot analysis of APP. Whole cell lysates from neuroblastoma cells immunoblotted as described in Materials and Methods, procedure 1 using MAB348 (A), and procedure 2 using 6E10 (B) and MAB348 (C). Figure Key: 0 h untreated extracts (10 µg); 24 h untreated extracts (10 µg); 24 h 10 µM DBPP (10 µg); Procedure 2 APP signals were calculated relative to β-actin signals (B, C).

Subsequently, the effect of 10 µM DBPP on the concentration of Aβ in the medium was determined using an ELISA assay (Millipore). In order to enhance the detection capabilities of the assay for Aβ peptides Aβ40 and Aβ42, culture media was concentrated in 2K VivaSpin columns and then analyzed by ELISA. In addition, the flow

through was assessed to verify that Aβ40 and Aβ42 did not elute through the filter. The untreated samples at 24 h contained 28.22 ± 1.04 pg of Aβ42 per mg of total protein and 133.69 ± 1.85 pg of Aβ40 per mg of total protein (Table 3). The samples treated with 10μM DBPP contained 140.99 ± 7.76 pg of Aβ42 per mg of total protein and 246.32 ± 6.63 pg of Aβ40 per mg of total protein. A significant increase in both peptides was observed for both Aβ40 and Aβ42 peptides in cells treated with DBPP.

TABLE 3. Quantification of Aβ Peptides

	Aβ 42 (pg/mg)	**Aβ 40 (pg/mg)**
0 h	9.39 ± 0.49	25.37 ± 1.31
24 h	28.22 ± 1.04	133.69 ± 1.85
DBPP	140.99 ± 7.76	246.32 ± 6.63

Expressed as pg Aβ per mg of protein. Data shown is the mean ± SEM (n=4).

CHAPTER 4

DISCUSSION

Although the primary role of BuChE neurodegenerative diseases is unknown, there appears to be an association between elevated BuChE activity and increased Aβ peptide synthesis (58). As such, additional research has focused on the role of BuChE in plaque formation. Others have shown that reversible inhibitors of the enzyme suppressed the formation of Aβ peptide (58). The hypothesis in this study is that irreversible inhibitors of BuChE might be more efficient inhibitors of Aβ peptide expression.

Reversible and irreversible inhibitors are dose-dependent, i.e. the effects of the drug are based upon their bioavailability and rate of elimination. Since the irreversible inhibitors described in this study covalently modify the catalytic serine of the enzyme (62), pharmacological effects may last longer in patients. Thus the advantages of targeting Aβ peptide formation with irreversible BuChE inhibitors are several: lesser and fewer side effects, longer pharmacological effects at a much lower dosage, and an extended period of time between necessary doses.

Previously, aryl dialkyl phosphates were shown to be potent, highly selective *irreversible* inhibitors of BuChE (50). Although these compounds are highly specific for BuChE, there is still possibility for interaction with other enzymes. To this end, a number of these aryl di-alkyl phosphates, including di-*n*-butyl 2-chlorophenyl phosphate (DBPP), were evaluated for their inhibitory activity on a number of enzymes. These

compounds were tested against AChE, which has a high degree of homology with BuChE, as well as the serine proteases, trypsin and chymotrypsin, which possess similar active sites to BuChE and were shown to have no inhibitory activity on these enzymes. Additionally, DBPP was tested against the kinases hexokinase, and PKA and had no inhibitory effect on these enzymes as well (62). This suggests that the off-target effects of the aryl dialkyl phosphates are minimal.

Although the concentration of DBPP used in this study is likely higher than what would be used clinically, the high non-lethal dosage used was to maximize the interaction between DBPP and BuChE and observe the pathological effect on the cells. Other studies using specific reversible inhibitors of BuChE also reported use of a higher concentration of compound without an effect in cell viability (58,64). But these studies only assessed LDH activity as a function of cell viability. It is difficult to compare the dosage requirements for cell culture studies and what would be used in clinical trials due to the fact that *in vitro* studies do not truly mimic the physiological state of the enzymes *in vivo* (64). The use of irreversible inhibitors, however, would require a much smaller dose than the current therapeutics used to treat AD. Although these compounds were shown to have little toxic effects on neuroblastoma cells, it was important to show that DBPP is actually taken up by the cells. An ideal inhibitor should have high blood-brain barrier permeability in order to interact with its target enzyme, BuChE. To this end, the efficiency of DBPP to cross the cellular membrane was measured.

The detection of DBPP from GC/MS analysis indicates that the compound does in fact accumulate within the cells, thus effectively crosses the cellular membrane. Others showed that DBPP does cross the blood brain barrier. Animals were injected with DBPP

and 30 minutes later the brains of rats were removed, homogenized, and extracted with dichloromethane. GC/MS analysis of the extracts detected considerable amounts of the compound (personal communication, Roger Acey). BuChE activity was reduced in brain homogenates treated with DBPP (65).

Preliminary data using confocal imagery suggests that BuChE is expressed on the plasma membrane, in the cytosol, and the nucleus (66). The presence of membrane-bound BuChE allows an immediate interaction with DBPP, which would account for the initial accumulation of DBPP detected. This indicates that the effects of the DBPP on BuChE are immediate, regardless of where the enzyme is expressed and that the compound has less potential to interact nonspecifically with other enzymes. The reduction in BuChE activity twenty-four hours post administration supports the inhibitory effect of DBPP on the enzyme.

The toxicity of DEPP on neuroblastoma cells as well as the compound's ability to cross the cellular membrane were analyzed. A ten-fold increase in the concentration of DEPP was required to see the same toxic effects as DBPP on the cells. However, GC/MS analysis revealed the lack of detectable DEPP accumulation, even twenty-four hours post administration. This suggests that the absence of DEPP accumulation in neuroblastoma cells was a result of its inability to diffuse across the cellular membrane, i.e., the reduced bioavailability is most likely due to its low hydrophobicity. Therefore, additional experiments measuring DEPP's effect on APP expression and Aβ formation were not conducted.

The effect of reversible BuChE inhibitors on Aβ production has been published. Greig et al. showed that neuroblastoma cells treated with a cymserine analog, PEC, a

reversible inhibitor of BuChE, resulted in a reduction of intracellular APP expression as well as in the amount of Aβ produced (58). Other studies demonstrated similar results. Phenserine or Tacrine, reversible inhibitors of BuChE, resulted in reduced expression of APP as well as a concomitant decrease in Aβ deposition in vitro (64,67,68). There is also evidence *in vivo* where there was a reduction in the Aβ deposition in transgenic mice overexpressing human APP (67). In this study, the initial assumption was that irreversible inhibitors of BuChE would inhibit Aβ peptide expression, similar to the effects of reversible inhibitors (58,64,67,68). In contrast, our results indicate that under the experimental conditions used in this study, DBPP exacerbates Aβ pathology. The immunoblot revealed that there was a reduction in the level of APP. There are several possibilities that may explain this observation. Increased Aβ secretion along with a reduction in intracellular APP levels suggests that DBPP may affect APP processing by regulating its synthesis or turnover. Shaw et al. demonstrated that Phenserine lowers the translational efficiency of APP mRNA (68). They discovered that Phenserine did not change APP mRNA levels, however, the change in APP protein levels was due to the drug interfering with the ribosomal subunit binding to the mRNA (68). There is evidence that Tacrine affects the trafficking of APP through the ER-Golgi pathway, attributing to reduced levels of the protein (64). Other groups have shown cholinesterase inhibitors target post-translational stages, such as glycosylation, phosphorylation, and secretion of APP (67). Defining the molecular mechanism in which DBPP interacts with the cellular processing of APP should be considered in subsequent studies.

There is evidence suggesting that cholinesterases interact with Aβ through non-catalytic domains, thus inhibitors binding to this site may interfere with the interaction

between cholinesterases and Aβ (69,70). In regards to this study, specific domains of BuChE to focus on would be the active site gorge and the C-terminal domain (CTD), which is associated with attenuating Aβ fibril formation (55). The CTD of BuChE is capable of forming heteroaromatic complexes with soluble monomeric Aβ; this interaction interferes with the β-sheet structure stabilization, thus attenuating fibrillization by inhibiting its aggregation to form toxic Aβ oligomers and fibrils (55). It is possible that excess DBPP may be interacting with BuChE at locations other than the active site, such as its CTD, or it may be that the binding of DBPP to BuChE may result in some conformational change within the CTD structure. Either of these events could disrupt the enzyme's association with Aβ, thereby resulting in impaired ability to attenuate fibril formation (55). This could possibly result in increased Aβ deposition, as the Aβ peptides may be more susceptible to β-sheet polymerization and fibrillization (37,51,53). Conformational studies would be beneficial to determine if interaction with this class of compounds causes structural changes within BuChE.

Increased amounts of Aβ resulting from inhibition of BuChE with higher concentrations of DBPP may also be the result of Aβ's ability to induce increased expression and processing of APP (49). This occurs through several processes. Aβ toxicity promotes the production of inflammatory molecules (TNF-α and IL-1β). These molecules have been reported to interact with APP promoter, thereby enhancing its production and processing to produce more Aβ species (46). Additionally, these molecules also upregulate expression of β-secretase, which in turn, leads to increased APP processing. The accumulation of Aβ peptides, generated by β-secretase, stimulates increased β-secretase synthesis and secretion. This would produce more Aβ peptides,

which would participate further in this positive feedback system to enhance the levels of Aβ peptides (49,69). Increased processing of APP could account for the reduced levels of this protein observed by western blot. Interestingly, preliminary studies in our lab showed that at lower concentrations of the inhibitor, normal levels of Aβ peptide expression were observed and decreased further by lowering the DBPP concentration (72). It is clear that the effect of the inhibitor is concentration dependent and there is a fine line between inhibiting BuChE and Aβ peptide formation.

The aryl dialkyl phosphates used in this study are highly specific irreversible BuChE inhibitors (50). The specificity of these compounds has been tested against numerous enzymes, but it is still possible that DBPP could interact with other enzymes. Studies investigating BuChE's potential interactions with related enzymes and those implicated in AD, such as α-, β-, and γ-secretase, would be important to help elucidate the molecular mechanisms involved in AD. It would be interesting to determine if changes in the expression levels of these secretases or the products are affected by a potential interaction with DBPP.

In this study, we did not attempt to differentiate among the various APP derivatives generated from α-, β-, and γ-secretase proteolysis. Subsequent studies evaluating the potential changes in the proteolytic fragments from these enzymes would be of interest; these could give further insight as to possible molecular interactions between BuChE and the enzymes involved in AD.

Future studies could be aimed at further elucidating DBPP's effect on Aβ peptide formation. It would be interesting to determine which species of Aβ form as the result of BuChE inhibition with DBPP. There are a variety of antibodies that recognize specific

forms of these amyloid species (i.e. monomers, oligomers, or fibrils) (73), which can be employed in ELISA assays, dot blots, and western blots to evaluate the changes, if any, of these different species. In this study, the extent of Aβ accumulation was only measured extracellularly, i.e., the peptides secreted in the media. However, Aβ is known to accumulate intracellularly as well (74); the peptide is cleaved within the cell by β-secretase and is not always secreted to the extracellular space (39). Determining the concentration of these species within neuroblastoma cells would aim to solve whether or not the effects of DBPP on Aβ are observed intracellularly, as well as extracellularly. Furthermore, the results of this study raise questions as to whether all irreversible inhibitors of BuChE result in increased Aβ concentrations, or if increased peptide formation is just an artifact from the compound. It may be that another similar compound may be more effective in reducing Aβ peptide accumulation. Future experiments will involve the use of slightly modified aryl di-alkyl phosphate compounds to evaluate the effect on Aβ production.

In summary, the data presented here provides insight into the relationship between BuChE inhibition and Aβ pathology and more specifically, the effect of irreversible inhibition of BuChE on APP and Aβ levels. Future studies would focus on whether the effect of irreversible inhibition with DBPP is specific or a more general occurrence affecting other proteins. The molecular mechanisms involved in AD are numerous and rarely straightforward. The cholinesterases, however, have been shown to associate with amyloid plaques, thus considerable effort has been directed toward developing compounds that target these enzymes to reduce Aβ load in AD. Those that target BuChE specifically have become increasingly popular, as this enzyme's activity is elevated in

AD. Even though there has been extensive research aiming to elucidate BuChE's exact role in AD, its function still remains unknown. It is certain that given the importance of this enzyme in AD, more studies are necessary to fully understand how inhibition of BuChE regulates Aβ pathology.

REFERENCES

REFERENCES

1. Chen, V. P., Xie, H. Q., Chan, W. K., Leung, K. W., Chan, G. K., Choi, R. C., Bon, S., Massoulie, J., and Tsim, K. W. (2010) The PRiMA-linked cholinesterase tetramers are assembled from homodimers: hybrid molecules composed of acetylcholinesterase and butyrylcholinesterase dimers are up-regulated during development of chicken brain. *J. Biol. Chem.* **285**, 27265-27278

2. Masson, P., Carletti, E., and Nachon, F. (2009) Structure, activities and biomedical applications of human butyrylcholinesterase. *Protein Pept. Lett.* **16**, 1215-1224

3. Nicolet, Y., Lockridge, O., Masson, P., Fontecilla-Camps, J. C., and Nachon, F. (2003) Crystal structure of human butyrylcholinesterase and of its complexes with substrate and products. *J. Biol. Chem.* **278**, 41141-41147

4. Johnson, G., and Moore, S. W. (2012) Why has butyrylcholinesterase been retained? Structural and functional diversification in a duplicated gene. *Neurochem. Int.* **61**, 783-797

5. Sridhar, G. R. (2012) Human butyrylcholinesterase knock-out equivalent: Potential to assess role in Alzheimer's disease. *Adv. Alzheimer Dis.* **1**, 1-11

6. Massoulie, J., Perrier, A., and Krejci, E. (2002) PRiMA: The membrane anchor of acetylcholinesterase in the brain. *Neuron* **33**, 275-285

7. Cokugras, N. (2003) Butyrylcholinesterase: Structure and physiological importance. *Turk. J. Neurochem.* **28**, 54-61

8. Giacobini, E. (2003) Cholinesterase: New roles in brain function and in Alzheimer's Disease. *Neurochem. Res.* **28**, 515-522

9. Darvesh, S., and Hopkins, D. A. (2003) Differential distribution of butyrylcholinesterase and acetylcholinesterase in the human thalamus. *J. Comp. Neurol.* **463**, 25-43

10. Mesulam, M., Guillozet, A., Shaw, P., Levey, A., Duysen, E. G., and Lockridge, O. (2002) Acetylcholinesterase knockouts establish central cholinergic pathways and can use butyrylcholinesterase to hydrolyze acetylcholine. *Neuroscience* **110**, 627-639

11. Darreh-Shori, T. (2006) Molecular changes of acetylcholinesterase and butyrlcholinesterase in Alzheimer patients during the natural course of the disease and treatment with cholinesterase inhibitors. Thesis for Doctoral degree (Ph.D.) Stockholm

12. Hartmann, J., Kiewert, C., Duysen, E. G., Lockridge, O., Greig, N. H., and Klein, J. (2007) Excessive hippocampal acetylcholine levels in acetylcholinesterase-deficient mice are moderated by butyrylcholinesterase activity. *J. Neurochem.* **100**, 1421-1429

13. Mack, A., and Robitzki, A. (2000) The key role of butyrylcholinesterase during neurogenesis and neural disorders: an antisense-5'butyrylcholinesterase-DNA study. *Prog. Neurobiol.* **60**, 607-628

14. Robitzki, A., Mack, A., Chattonet, A., and Layer, P. G. (1997) Transfection of reaggregating embryonic chicken retinal cells with antisense 5'-DNA butyrylcholinesterase expression vector inhibits proliferations and alters neurogenesis. *J. Neurochem.* **69**, 823-833

15. Johnson, G., and Moore, S. W. (2000) Cholinesterases modulate cell adhesion in human neuroblastoma cells in vitro. *Int. J. Devl. Neurosci.* **18**, 781-790

16. Robitzki, A., Mack, A., Hoppe, U., Chattonet, A., and Layer, P. G. (1997) Regulation of cholinesterase gene expression affects neuronal differentiation revealed by transfection studies on reaggregating embryonic chicken retinal cells. *Eur. J. Neurosci.* **9**, 2394-2405

17. Layer, P. G., Weikert, T., and Alber, R. (1993) Cholinesterases regulate neurite growth of chick nerve cells in vitro by means of a non-enzymatic mechanism. *Cell Tissue Res.* **273**, 219-226

18. Paraoanu, L. E., Steinert, G., Koehler, A., Wessler, I., and Layer, P. G. (2007) Expression and possible functions of the cholinergic system in a murine embryonic stem cell line. *Life Sci.* **80**, 2375-2379

19. Layer, P. G., Alber, R., and Sporns, O. (1987) Quantitative development and molecular forms of acetyl- and butyrylcholinesterase during morphogenesis and synaptogenesis of chick brain and retina. *J. Neurochem.* **49**, 175-182

20. Sperling, L. E., Steinert, G., Boutter, J., Landgraf, D., Hescheler, J., Pollet, D., and Layer, P. G. (2008) Characterisation of cholinesterase expression during murine embryonic stem cell differentiation. *Chem. Biol. Interact.* **175**, 156-160

21. Patinkin, D., Seidman, S., Eckstein, F., Benseler, F., Zakut, H., and Soreq, H. (1990) Manipulations of cholinesterase gene expression modulate murine megakaryocytopoiesis in vitro. *Mol. Cell Biol.* **10**, 6046-6050

22. Shankar, G. M., Bloodgood, B. L., Townsend, M., Walsh, D. M., Selkoe, D. J., and Sabatini, B. L. (2007) Natural oligomers of the Alzheimer amyloid-beta protein induce reversible synapse loss by modulating an NMDA-type glutamate receptor-dependent signaling pathway. *J. Neurosci.* **27**, 2866-2875

23. Tomiyama, T., Matsuyama, S., Iso, H., Umeda, T., Takuma, H., Ohnishi, K., Ishibashi, K., Teraoka, R., Sakama, N., Yamashita, T., Nishitsuji, K., Ito, K., Shimada, H., Lambert, M. P., Klein, W. L., and Mori, H. (2010) A mouse model of amyloid beta oligomers: Their contribution to synaptic alteration, abnormal tau phosphorylation, glial activation, and neuronal loss in vivo. *J. Neurosci.* **30**, 4845-4856

24. Alzheimer's Disease Education & Referral (ADEAR) Center: Alzheimer's Disease Fact Sheet 2013. *National institute on Aging, NIH*

25. Venugopal, C., Demos, C., Jagannatha, K., Pappolla, M., and Sambamurti, K. (2008) Beta-secretase: Structure, function, and evolution. *CNS Neurol. Disord. Drug Targets* **7**, 278-294

26. Cole, S. L., and Vassar, R. (2008) The role of amyloid precursor protein processing by BACE1, the beta-secretase, in Alzheimer Disease pathophysiology. *J. Biol. Chem.* **283**, 29621-29625

27. Hardy, J., and Selkoe, D. J. (2002) The amyloid hypothesis of Alzheimer's disease: progress and problems on the road to therapeutics. *Science* **297**, 353-356

28. Bali, J., Halima, S., Felmy, B., Goodger, Z., Zurbriggen, S., and Rajendran, L. (2010) Cellular basis of Alzheimer's Disease. *Ann. Ind. Acad. Neurol.* **13**, 89-93

29. Haass, C., Kaether, C., Thinakaran, G., and Sisodia, S. (2012) Trafficking and proteolytic processing of APP. *Cold Spring Harb. Perspect. Med.* **2**, a006270

30. Zheng, H., and Koo, E. H. (2006) The amyloid precursor protein: beyond amyloid. *Mol. Neurodegener.* **1**: 5

31. Allinquant, B., Hantraye, P., Mailleux, P., Moya, K. L., Bouilloy, C., and Prochiantz, A. (1995) Downregulation of ayloid protein inhibits neurite outgrowth in vitro. *J. Cell Biol.* **128**, 919-927

32. Herard, A. S., Besret, L., Dubois, A., Dauguet, J., Delzescaux, T., Hantraye, P., Bonvento, G., and Moya, K. L. (2006) siRNA targeted against amyloid precursor protein impairs synaptic activity in vivo. *Neurobiol. Aging* **27**, 1740-1750

33. Lichtenthaler, S. F., Haass, C., and Steiner, H. (2011) Regulated intramembrane proteolysis--lessons from amyloid precursor protein processing. *J. Neurochem.* **117**, 779-796

34. Vingtdeux, V., Sergeant, N., and Buee, L. (2012) Potential contribution of exosomes to the prion-like propagation of lesions in Alzheimer's disease. *Front. Physiol.* **3**: 229

35. Dislich, B., and Lichtenthaler, S. F. (2012) The membrane-bound aspartyl protease BACE1: Molecular and functional properties in Alzheimer's Disease and beyond. *Front. Physiol.* **3**: 8

36. Fluhrer, R., Steiner, H., and Haass, C. (2009) Intramembrane proteolysis by signal peptide peptidases: a comparative discussion of GXGD-type aspartyl proteases. *J. Biol. Chem.* **284**, 13975-13979

37. Xu, Y., Shen, J., Luo, X., Zhu, W., Chen, K., Ma, J., and Jiang, H. (2005) Conformational transition of amyloid beta-peptide. *Proc. Natl. Acad. Sci. USA* **102**, 5403-5407

38. Bieschke, J., Herbst, M., Wiglenda, T., Friedrich, R. P., Boeddrich, A., Schiele, F., Kleckers, D., Lopez del Amo, J. M., Gruning, B. A., Wang, Q., Schmidt, M. R., Lurz, R., Anwyl, R., Schnoegl, S., Fandrich, M., Frank, R. F., Reif, B., Gunther, S., Walsh, D. M., and Wanker, E. E. (2012) Small-molecule conversion of toxic oligomers to nontoxic beta-sheet-rich amyloid fibrils. *Nat. Chem. Biol.* **8**, 93-101

39. Rajendran, L., Honsho, M., Zahn, T. R., Keller, P., Geiger, K. D., Verkade, P., and Simons, K. (2006) Alzheimer's disease beta-amyloid peptides are released in association with exosomes. *Proc. Natl. Acad. Sci. USA* **103**, 11172-11177

40. Kaether, C., Schmitt, S., Willem, M., and Haass, C. (2006) Amyloid precursor protein and Notch intracellular domains are generated after transport of their precursors to the cell surface. *Traffic* **7**, 408-415

41. Shimizu, H., Tosaki, A., Kaneko, K., Hisano, T., Sakurai, T., and Nukina, N. (2008) Crystal structure of an active form of BACE1, an enzyme responsible for amyloid beta protein production. *Mol. Cell. Biol.* **28**, 3663-3671

42. Pelchen-Matthews, A., Raposo, G., and Marsh, M. (2004) Endosomes, exosomes and Trojan viruses. *Trends Microbiol.* **12**, 310-316

43. Aguzzi, A., and Rajendran, L. (2009) The transcellular spread of cytosolic amyloids, prions, and prionoids. *Neuron* **64**, 783-790

44. Cheng, I. H., Scearce-Levie, K., Legleiter, J., Palop, J. J., Gerstein, H., Bien-Ly, N., Puolivali, J., Lesne, S., Ashe, K. H., Muchowski, P. J., and Mucke, L. (2007) Accelerating amyloid-beta fibrillization reduces oligomer levels and functional deficits in Alzheimer disease mouse models. *J. Biol. Chem.* **282**, 23818-23828

45. Lacor, P. N., Buniel, M. C., Furlow, P. W., Clemente, A. S., Velasco, P. T., Wood, M., Viola, K. L., and Klein, W. L. (2007) Abeta oligomer-induced aberrations in synapse composition, shape, and density provide a molecular basis for loss of connectivity in Alzheimer's disease. *J. Neurosci.* **27**, 796-807

46. Akiyama, H. (2006) Abeta, tau, and alpha-synuclein and glial cells. *Nihon Shinkei Seishin Yakurigaku Zasshi* **26**, 23-31

47. Borghi, R., Patriarca, S., Traverso, N., Piccini, A., Storace, D., Garuti, A., Cirmena, G., Odetti, P., and Tabaton, M. (2007) The increased activity of BACE1 correlates with oxidative stress in Alzheimer's Disease. *Neurobiol. Aging* **28**, 1009-1014

48. Tamagno, E., Parola, M., Bardini, P., Piccini, A., Borghi, R., Guglielmotto, M., Santoro, G., Davit, A., Danni, O., Smith, M., Perry, G., and Tabaton, M. (2005) Beta-site APP cleaving enzyme upregulation induced by 4-hydroxynonenal is mediated by stress-activated protein kinase pathways. *J. Neurochem.* **92**, 628-636

49. Tabaton, M., Zhu, X., Perry, G., Smith, M. A., and Giliberto, L. (2010) Signaling effect of amyloid-beta(42) on the processing of AbetaPP. *Exp.l Neurol.* **221**, 18-25

50. Law, K. S., Acey, R. A., Smith, C. R., Benton, D. A., Soroushian, S., Eckenrod, B., Stedman, R., Kantardjieff, K. A., and Nakayama, K. (2007) Dialkyl phenyl phosphates as novel selective inhibitors of butyrylcholinesterase. *Biochem. Biophys. Res. Commun.* **355**, 371-378

51. Inestrosa, N. C., Dinamarca, M. C., and Alvarez, A. (2008) Amyloid-cholinesterase interactions. Implications for Alzheimer's disease. *FEBS J.* **275**, 625-632

52. Bartolini, M., Bertucci, C., Cavrini, V., and Andrisano, V. (2003) Beta-Amyloid aggregation induced by human acetylcholinesterase: inhibition studies. *Biochem. Pharmacol.* **65**, 407-416

53. Inestrosa, N. C., Alvarez, A., perez, C., Moreno, R., Vicente, M., Linker, C., Casanueva, O., Soto, C., and Garrido, J. (1996) Acetylcholinesterase accelerates assembly of amyloid-beta-peptides into Alzheimer's fibrils: Possible role of the peripheral site of the enzyme. *Neuron* **16**, 881-891

54. Dinamarca, M. C., Sagal, J. P., Quintanilla, R. A., Godoy, J. A., Arrazola, M. S., and Inestrosa, N. C. (2010) Amyloid-beta-Acetylcholinesterase complexes potentiate neurodegenerative changes induced by the Abeta peptide. Implications for the pathogenesis of Alzheimer's disease. *Mol. Neurodegener.* **5**: 4

55. Diamant, S., Podoly, E., Friedler, A., Ligumsky, H., Livnah, O., and Soreq, H. (2006) Butyrylcholinesterase attenuates amyloid fibril formation in vitro. *Proc. Natl. Acad. Sci. USA* **103**, 8628-8633

56. Arendt, T., Bruckner, M. K., lange, M., and Bigl, V. (1992) Changes in acetylcholinesterase and butyrylcholinesterase in Alzheimer's Disease resemble embryonic development--a study of molecular forms. *Neurochem. Int.* **21**, 381-396

57. Podoly, E., Hanin, G., and Soreq, H. (2010) Alanine-to-threonine substitutions and amyloid diseases: butyrylcholinesterase as a case study. *Chem. Biol. Interact.* **187**, 64-71

58. Greig, N. H., Utsuki, T., Ingram, D. K., Wang, Y., Pepeu, G., Scali, C., Yu, Q. S., Mamczarz, J., Holloway, H. W., Giordano, T., Chen, D., Furukawa, K., Sambamurti, K., Brossi, A., and Lahiri, D. K. (2005) Selective butyrylcholinesterase inhibition elevates brain acetylcholine, augments learning and lowers Alzheimer beta-amyloid peptide in rodent. *Proc. Natl. Acad. Sci. USA* **102**, 17213-17218

59. Pohanka, M. (2011) Cholinesterases, a target of pharmacology and toxicology. *Biomed. Pap. Med. Fac. Univ. Palack Olomouc, Czech. Repub.* **155**, 219-229

60. Mikiciuk-Olasik, E., Szymanski, P., and Zurek, E. (2007) Diagnostics and therapy of Alzheimer's Disease. *Ind. J. Exp.l Biol.* **45**, 315-325

61. Cerbai, F., Giovannini, M. G., Melani, C., Enz, A., and Pepeu, G. (2007) N1phenethyl-norcymserine, a selective butyrylcholinesterase inhibitor, increases acetylcholine release in rat cerebral cortex: a comparison with donepezil and rivastigmine. *Eur. J. Pharmacol.* **572**, 142-150

62. MacArthur, C. C. (2008) Dialkyl chlorophenyl phosphates: Selective inhibitors of butyrylcholinesterase. Thesis for Master's Degree (M.Sc.) *CSULB*

63. Slunt, H. H., Thinakaran, G., Von Koch, C., Lo, A., Tanzi, R., and Sisodia, S. (1994) Expression of a ubiquious, cross-reactive homologue of the mouse beta-amyloid precursor protein (APP). *J. Biol. Chem.* **269**, 2637-2644

64. Lahiri, D. K., Farlow, M. R., and Sambamurti, K. (1998) The secretion of amyloid-beta peptides is inhibited in the tacrine-treated human neuroblastoma cells. *Mol. Brain Res.* **62**, 131-140

65. Del Cid, J.S., Cage, F.M., Poynter, S.T., MacArthur, C., Nakayama, K., and Acey, R. (2012) Aryl dialkyl phosphate inhibitors of butyrylcholinesterase as potential therapeutics for Alzheimer's Disease: Characterization of off-target effects. Poster Presentation, CSULB

66. Kunicki, M., Mana, W., and Acey, R.A., Butyrylcholinesterase expression in Developing Neural Tissue. CSUPERB Meeting, Jan. 3-5, 2013, Anaheim, CA.

67. Lahiri, D. K., Farlow, M. R., Hintz, N., Utsuki, T., and Greig, N. H. (2000) Cholinesterase inhibitors, beta-amyloid precursor protein and amyloid-Beta peptides in Alzheimer's Disease. *Acta. Neurol. Scand*. **176**, 60-67

68. Shaw, K. T., Utsuki, T., Rogers, J., Yu, Q. S., Sambamurti, K., Brossi, A., Ge, Y. W., Lahiri, D. K., and Greig, N. H. (2001) Phenserine regulates translation of beta - amyloid precursor protein mRNA by a putative interleukin-1 responsive element, a target for drug development. *Proc. Natl. Acad. Sci. USA* **98**, 7605-7610

69. Kozurkova, M., Hamulakova, S., Gazova, Z., Paulikova, H., and Kristian, P. (2011) Neuroactive Multifunctional Tacrine Congeners with Cholinesterase, Anti-Amyloid Aggregation and Neuroprotective Properties. *Pharmaceuticals* **4**, 382-418

70. Bolognesi, M. L., Cavalli, L., Valgimigli, L., Bartolini, M., Rosini, M., Andrisano, V., Recanatini, M., and Melchiorre, C. (2007) Multi-target directed drug design strategy: From a dual binding site acetylcholinesterase inhibitor to a trifunctional compound against Alzheimer's Disease. *J. Med. Chem.* **50**, 6446-6449

71. Silveyra, M., Garcia-Ayllon, M., Serra-Basante, C., Mazzoni, V., Garcia-Gutierrez, M., Manzanares, J., Culvenor, J. G., and Saez-Valero, J. (2012) Changes in acetylcholinesterase expression are associated with altered presenilin-1 levels. *Neurobiol. Aging* **33**, 27-37

72. Turner, A. (2013) Effects of Di-n-Butyl-2-Chlorophenyl Phosphate on amyloid-beta 40 & 42 Formation. Poster presentation, CSULB.

73. Kayed, R., Canto, I., Breydo, L., Rasool, S., Lukacsovich, T., Wu, J., Albay, R., Pensalfini, A., Yeung, S., Head, E., March, J. L., and Glabe, C. G. (2010) Conformation dependent monoclonal antibodies distinguish different replicating strains or conformers of prefibrillar Abeta oligomers. *Mol. Neurodegener.* **5**, 57

74. Gouras, G. K., Tsai, J., Naslund, J., Vincent, B., Edgar, M., Checler, F., Greenfield, J. P., Haroutunian, V., Buxbaum, J. D., Xu, H., Greengard, P., and Relkin, N. R. (2000) Intraneuronal Aβ42 accumulation in human brain *Am. J. Pathol.* **156**, 15-20